DETERMINISTIC COASTAL MORPHOLOGICAL AND SEDIMENT TRANSPORT MODELING: A REVIEW AND DISCUSSION

Laurent O. Amoudry[1] and Alejandro J. Souza[1]

[1]   Modern coastal ocean modeling systems are now capable of numerically simulating a variety of coastal and estuarine problems and can thus provide useful information for managing coastal zones. Here we review state-of-the-art Eulerian implementations of bottom-up sediment transport and morphological change in coastal ocean hydrodynamic models. In order to investigate the fate of suspended sediment in coastal and estuarine waters as well as the evolution of sea or river beds, sediment dynamics need to be represented at a scale relevant to the numerical discretized solution, and significant effort is devoted to parameterize sediment processes. We discuss boundary layer hydrodynamics and the computation of the bed shear stress. We also focus on approaches used to represent near-bed processes such as bed load transport and sediment erosion and deposition. Sediment diffusivities, settling velocities, and cohesive processes such as flocculation all have an impact on suspended sediment throughout the water column. We then describe the implementation of process parameterizations in coastal hydrodynamic models, explicitly reviewing five widely used systems. The approaches implemented in these coastal models may present distinct strengths and shortcomings with regard to some important issues for coastal zones, both numerical and physical. While these detailed limitations need to be considered as part of model assessment, more general issues also hinder present state-of-the-art models. In particular, sediment transport is inherently highly empirical, which is further compounded by issues arising from turbulence closure schemes. We conclude by suggesting some possible directions toward improving sediment dynamics understanding and coastal-scale predictive ability.

1. INTRODUCTION

[2] Appropriate modeling tools are crucial to the management of nearshore and estuarine areas. The importance of sediment dynamics in coastal interactions further emphasizes the need for sediment transport and morphodynamic modeling. Morphological models can generally be classified into process-based or behavior-based models. The first approach is based on representing all relevant sediment transport processes. The second approach implements simple parameterized descriptions of the general behavior of the morphological system at the larger scales of interest (centennial to geological) and relies essentially on long-term data sets for calibration. *De Vriend et al.* [1993] also classified morphological models in four categories on the basis of spatial scales and dimensions. "Coastline models" integrate over all small scales and only describe the largest-scale long-shore behavior. "Coastal profile models" ignore the long-shore variation and concentrate on the cross-shore evolution. These models usually consider the vertical and the cross-shore dimensions and are thus usually referred to as two-dimensional vertical (2DV) models [e.g., *Zhang et al.*, 1999; *Harris and Wiberg*, 2001; *Hsu et al.*, 2006]. "Coastal area models," which are the focus of the present review, include both horizontal dimensions and can either be depth-averaged or resolve vertical variations in fully three-dimensional models. Finally, "local models" focus on small-scale phenomena (e.g., bottom boundary layer processes, rippled bed regime transport, and sheet flows) and ignore larger scales.

[3] We focus here on deterministic (i.e., process-based) coastal ocean models, which are being increasingly used to study coastal sediment dynamics and coastal morphological evolution [e.g., *Lumborg*, 2005; *Blaas et al.*, 2007; *Souza et al.*, 2007; *Zanuttigh*, 2007; *Harris et al.*, 2008; *Brown and Davies*, 2009; *Hu et al.*, 2009]. These models usually treat the short-term (hours to days) to medium-term (days

[1]National Oceanography Centre, Liverpool, UK.

to months) evolution. Historically, they were first based on depth-averaged equations (two-dimensional horizontal (2DH) models) and were applied both to riverine [*Struiksma et al.*, 1985] and coastal [*de Vriend*, 1987] environments. The important concepts were reviewed by *de Vriend et al.* [1993] and such approaches are still employed both in riverine [*Wu*, 2004] and coastal [*Cookman and Flemings*, 2001; *Damgaard et al.*, 2002] environments. However, 2DH approaches have limited applicability and in many situations the three-dimensional flow structure has to be described. In such cases, quasi three-dimensional (quasi 3-D) concepts were developed and added to 2DH models to avoid solving the full three-dimensional hydrodynamic equations [*de Vriend and Ribberink*, 1988; *Briand and Kamphuis*, 1993; *Roelvink et al.*, 1994; *Elfrink et al.*, 1996]. Models have now also recently turned to solving the full three-dimensional equations both for river applications [*Gessler et al.*, 1999; *Wu et al.*, 2000; *Fang and Rodi*, 2003] and for coastal environments [*Lesser et al.*, 2004; *Wai et al.*, 2004; *Warner et al.*, 2008].

[4] Coastal ocean modeling systems typically consist of a modular structure. The core of this structure is a hydrodynamic model to which wave models, turbulence models, ecosystem models, and sediment models can be added. While all these models are interlinked, sediment dynamics are usually implemented as depending more on the hydrodynamics, waves, and turbulence than vice versa. The global outputs and model products reflect this modular structure and cover a wide range of coastal processes and dynamics. The sediment models typically aim to predict the full three-dimensional suspended sediment concentration as well as the two-dimensional bed evolution. For the obvious reason of computational cost, current models cannot resolve the scales of the smallest physical processes. In particular, flow turbulence, near-bed dynamics, and intrawave processes are resolved neither lengthwise nor timewise. Appropriate parameterization of such small-scale processes is thus crucial to the representation of coastal and estuarine dynamics and represents most of the research associated with sediment transport and coastal hydrodynamics.

[5] Sediment particles initiate motion when the moments of the driving forces about a contact point exceed the stabilizing moments. Grains then roll, slide, and jump along the bed, resulting in bed load transport. If the lift forces, with the assistance of the turbulent eddies, exceed the grain weight, sediment particles may be entrained into suspension. It is customary to keep a distinction between bed load and suspended load for all driving conditions as they correspond to different physical mechanisms. Bed load occurs in a thin region of high concentration near the bed and is primarily due to interparticle interactions. In contrast, suspended load occurs higher in the water column and results from the agitation of fluid turbulence. This distinction is also related to the concept of the total water-sediment mixture stress being split in two parts [*Bagnold*, 1954], one part transmitted by the fluid and one part transmitted by the interparticle interactions. While this sediment-transmitted shear stress is now commonly included in some small-scale sed-

iment modeling (e.g., *Ahilan and Sleath* [1987] and *Hsu et al.* [2004] for one-dimensional sheet flows and *Amoudry and Liu* [2009] for two-dimensional scouring), it is still neglected in coastal area models as being a small-scale very near bed process.

[6] Once sediment grains are transported, the sediment bed may deform because of a series of erosional and depositional events. At a relatively small scale, this leads to bed waves that have a significant impact on flow and sediment patterns. In particular, they increase the bed resistance to the flow by inducing form drag. The motion of individual particles at the bed is driven by skin friction, and form drag thus directly controls neither bed load nor erosion. However, form drag significantly modifies near-bed hydrodynamics and turbulence, which eventually feed back to sediment transport. Typical coastal area models focus on morphological patterns at a larger scale and do not resolve this small-scale morphology, which then has to be parameterized appropriately.

[7] Overall, sediment transport is a complex, multidimensional, and dynamic process that results from the interactions of coastal hydrodynamics, turbulence, and sediment particles. Grains can be transported by currents (tide driven, density driven, wave driven, or wind driven), wave motions, and combinations of the two. This movement of sediment can be investigated by numerically following the path of a number of discrete particles in Lagrangian models [e.g., *Lane*, 2005]. Eulerian models instead treat sediment as a continuum, and the presence of particles in suspension is represented by a concentration. We focus here on the latter approach, and we only review methods commonly implemented in coastal ocean modeling systems to predict sediment transport and morphological evolution. In general, biological effects on sediment dynamics are still not implemented in coastal area sediment transport models and are thus only briefly addressed, with the exception of bioturbation. Similarly, swash zone dynamics [e.g., *Brocchini and Baldock*, 2008] are not considered in the models we review. Even though coastal sediment transport is closely linked to a number of coastal hydrodynamic processes, we will not address these, other than the calculation of the bed shear stress. Despite the link between turbulence modeling and the vertical structure of suspended sediment, we also do not aim to provide a detailed description of all available turbulence closures in coastal ocean models. Finally, even though most modeling of sediment processes is empirically driven, we will not specifically discuss how new experimental techniques enable greater model sophistication and accuracy.

[8] We will first introduce the governing equations for sediment transport in coastal area models and discuss the implementations of appropriate boundary conditions. Because of the different scales involved, a number of physical sediment processes need to be parameterized. Focus is given to how the shear stress is computed and then to how bed load, sediment erosion, and deposition are represented. Descriptions of sediment turbulent diffusion, sediment settling, and cohesive processes are also discussed. We then address the implementation of the process models in coastal area systems and introduce
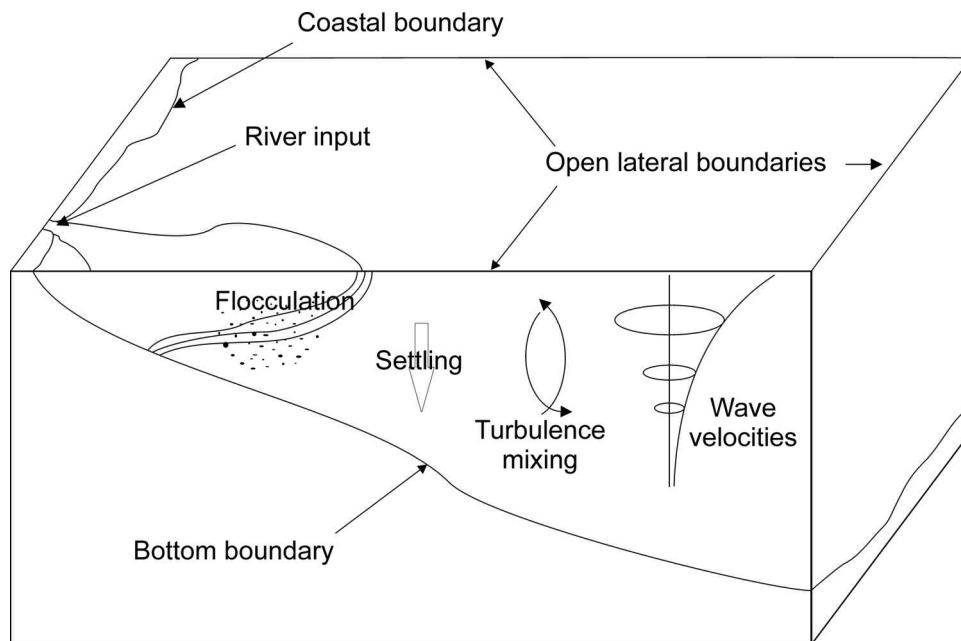
Figure 1. Coastal shelf sediment transport processes and boundaries. Lateral boundaries can be open or closed (coastal or river in this case).

five widely used recent systems. While our aim is not to promote any given model, the relative merits of different specific numerical and physical approaches, as well as the restrictions they may entrain, are examined. More general limitations on sediment transport modeling, such as empiricism and turbulence closures, are then discussed. Finally, we conclude with presenting future perspectives with the aim of improving our understanding of sediment processes and our predictive ability.

2. MATHEMATICAL FORMULATION OF SEDIMENT TRANSPORT IN REGIONAL MODELS

2.1. Governing Equations of Large-Scale Sediment Transport and Morphological Change

[9] Because of the vertical scales involved, regional models do not resolve the near-bed, high-concentration region, which is typically less than a few centimeters high. As such, the models implicitly assume a dilute mixture of sediment and water for which equations of motion are solved. In the coastal zone, water density variations due to salinity, temperature, and pressure are often accounted for, and the additional effect of sediment in suspension can be included as follows:

$$\rho = \rho_w + c_{vol}(\rho_s - \rho_w), \qquad (1)$$

where ρ is the density of the sediment-water mixture, ρ_s is the sediment particle density, ρ_w is the density of clear water (function of temperature, salinity, and pressure following the *Unesco* [1981] equation of state), and c_{vol} is the volumetric sediment concentration.

[10] Although we do not explicitly introduce them, the hydrodynamic governing equations are based on the principle of conservation of matter under some simplifying assumptions. Since flows in coastal environments are tur-

bulent and the models cannot resolve all turbulence scales, Reynolds averaging is usually applied to the governing equations.

[11] Calculations of both suspended sediment concentration and bed evolution are based on the basic principle of conservation of sediment mass. In the fluid flow, this principle, applied to an elemental volume, leads, after turbulent averaging, to a governing equation for the sediment concentration c, which typically reduces to an advection-diffusion equation of the following type:

$$\frac{\partial c}{\partial t} + \nabla \cdot (\vec{u}c) = \frac{\partial W_s c}{\partial z} + \nabla \cdot (K_c \nabla c) + S_c, \qquad (2)$$

where ∇ is the three-dimensional gradient operator, c is the sediment concentration, t is time, and $\vec{u}$ is the flow velocity vector. The left-hand-side terms represent the time rate of change in the concentration of suspended sediment and the rate of change of concentration due to advective fluxes, respectively. W_s is the settling velocity of sediment, and z is the vertical coordinate; the corresponding term represents the rate of change of sediment concentration due to the settling fluxes. The turbulent diffusive fluxes are modeled following the gradient diffusion hypothesis and are thus included in the $\nabla \cdot (K_c \nabla c)$ term, which represents the change of concentration due to diffusive fluxes. K_c is the sediment total diffusivity accounting both for molecular and turbulent diffusion. Finally, S_c is a possible sediment source/sink term. Appropriate boundary conditions and expressions for the settling velocity and sediment diffusivity (Figure 1) are needed to solve this equation and are discussed in following sections.

[12] Continuity of mass applied to an elemental area of the bed results in a governing equation for the bed elevation
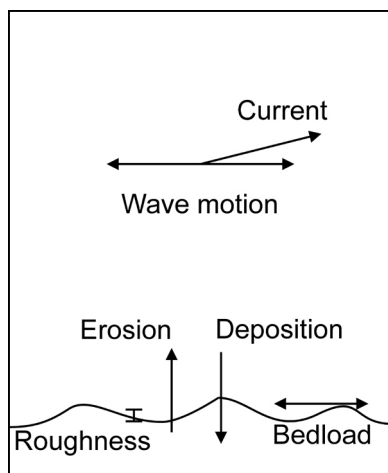
Figure 2. Near-bed sediment transport processes.

which is often referred to as the Exner equation. While a general form can be mathematically derived by considering the sediment balance in an arbitrary layer [e.g., *Paola and Voller*, 2005], simplified formulations are usually employed in coastal models. The mass balance of sediment can be applied to the entire water column [e.g., *Zhang et al.*, 1999; *Wu et al.*, 2000; *Harris and Wiberg*, 2001], but most three-dimensional models now consider this balance as applied to a near-bed layer and use

$$\rho_s(1 - p_c)\frac{\partial \eta_b}{\partial t} + \nabla_H \cdot \vec{Q}_B + E - D = 0, \qquad (3)$$

where ∇_H is the two-dimensional horizontal gradient (i.e., $(\partial/\partial x, \partial/\partial y, 0)$ in Cartesian coordinates). The variable η_b represents the bed location, E is the sediment erosion flux, D is the deposition flux, $\vec{Q}_B$ is the bed load transport rate vector, and p_c is the bed porosity [e.g., *Gessler et al.*, 1999]. These two governing equations are coupled through the sum of the erosion and deposition fluxes, which appears in the advection-diffusion equation either as a bottom boundary condition (Figure 2) or as a source/sink term for the bottom grids.

2.2. Boundary Conditions

[13] Appropriate boundary conditions are necessary for lateral, top, and bottom boundaries to solve the suspended sediment equation (equation (2)). Lateral boundary conditions (Figure 1) are commonly separated into closed boundaries, for which a free-slip or no-flux condition is used, and open boundaries, for which several options such as prescribed water level, normal velocity, and discharge exist. Large-scale coastal models commonly do not resolve the surf and swash zones, and the shoreline boundary is instead usually taken to be of the closed type [e.g., *Lesser et al.*, 2004; *Blaas et al.*, 2007], which may include a source term.

[14] At the top boundary (free surface), a flux condition is commonly used: either the total sediment flux [e.g., *Zhang et al.*, 1999; *Harris and Wiberg*, 2001] or the vertical dif-

fusive flux only [e.g., *Lesser et al.*, 2000] is set to vanish. At the bottom boundary, the condition can specify either the concentration value or the sediment vertical flux.

[15] The concentration boundary condition, also called reference concentration, provides a formula for the concentration at some reference level, that is, C_{ref} at z_{ref}, where both C_{ref} and z_{ref} are functions of flow and sediment parameters such as the Shields parameter (nondimensional bed shear stress), the sediment specific gravity, and the sediment diameter (C_{ref} is reference concentration and z_{ref} is reference location). An issue with this approach is that the bottom grid location may not coincide with the reference level, in which case the concentration at the bottom grid location needs to be extrapolated from the reference concentration, usually by means of a Rouse profile [*Lesser et al.*, 2000]. Many reference concentration relationships have been introduced, eight of which were assessed by *Garcia and Parker* [1991], and the most commonly used formulas in large-scale models remain those of *Smith and McLean* [1977] and *van Rijn* [1984a].

[16] Flux boundary conditions aim to provide some kind of information on the vertical sediment flux at the bottom boundary. Either the net sediment flux at the bottom boundary is specified directly as a boundary condition [e.g., *Harris and Wiberg*, 2001; *Wai et al.*, 2004], or erosion and deposition act as source and sink in the advection-diffusion equation and the diffusive (and advective) flux of sediment is set to zero at the bottom boundary [e.g., *Lesser et al.*, 2000; *Warner et al.*, 2008]. It has to be noted that whichever boundary condition approach is employed, the bed evolution equation (equation (3)) requires the specification of the bottom vertical fluxes (i.e., erosion and deposition), which is discussed in more detail in section 3.3.

3. MODELING SEDIMENT TRANSPORT PHYSICAL PROCESSES

3.1. Bottom Boundary Layer

[17] The thickness of the wave boundary layer is typically of the order of 10 cm. The vertical resolution of regional-scale models is thus not sufficient to resolve the near-bed fluid flow gradients, so algorithms that parameterize the bottom boundary layer processes are required. Individual waves are also not resolved timewise, and the boundary layer model then needs to provide some information on the bed shear stress without fully considering the intrawave result. As mentioned previously, from a hydrodynamic and turbulence point of view, the bed shear stress needs to account for skin friction and form drag. However, only the skin friction part should be considered as driving bed load transport and sediment erosion.

3.1.1. Current Boundary Layer

[18] The bottom shear stress for a pure current is commonly calculated using simple drag coefficient expressions, which in turn rely on linear bottom drag, quadratic bottom drag, or a logarithmic velocity profile. The first two approaches relate the bottom shear stress to the near-bed velocity through constant drag coefficients. The logarithmic approach, which can also be rewritten in a quadratic form, assumes that the
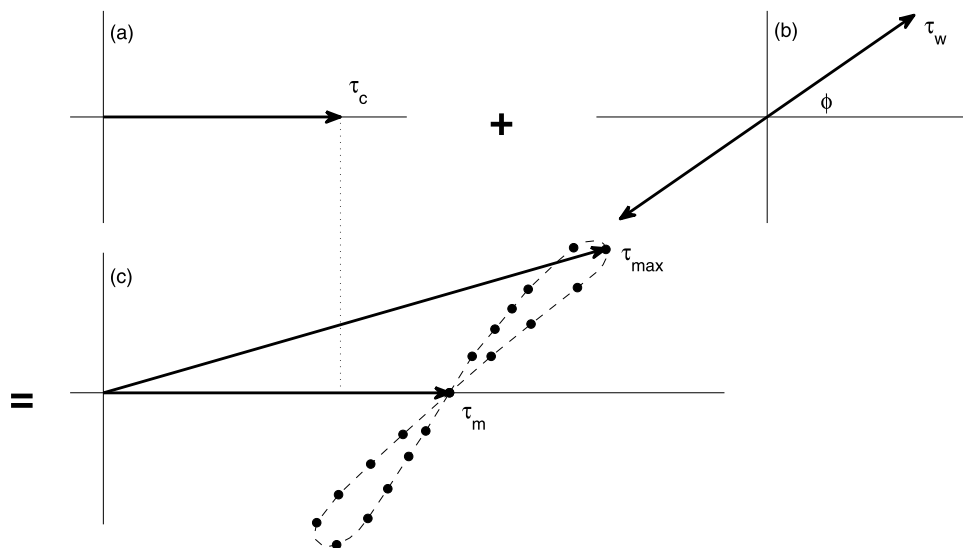
Figure 3. Bed shear stress with wave-current interaction [after *Soulsby et al.*, 1993]. The current-only stress τ_c and the wave-only stress of amplitude τ_w combine into the wave-current stress of mean τ_m ($\tau_m > \tau_c$) and maximum τ_{max}.

flow velocity follows the classic rough wall log law vertical profile close to the bed, for which the velocity at a given elevation is given by

$$u(z) = \frac{u_*}{\kappa} \ln\left(\frac{z}{z_0}\right), \qquad (4)$$

where $u_* = \sqrt{\tau_b/\rho_f}$ is the friction velocity, z_0 is the bed roughness length, and κ is the von Karman constant. A significant advantage of the log law approach with respect to constant drag coefficients is the dependence on the vertical distance from the bed, which is important when morphological changes are considered. An appropriate value for κ also has to be specified, and the clear fluid value of 0.41 is usually used. The specification of the roughness length will be discussed in more detail in section 3.1.3.

3.1.2. Wave and Wave-Current Boundary Layer

[19] Most bottom boundary layer models use the concept of a friction factor f_w to describe the wave-only bottom shear stress through a quadratic friction law, both for pure waves and combined wave-current cases:

$$\tau_w = \frac{1}{2} \rho f_w u_b^2, \qquad (5)$$

where u_b is the wave bottom orbital velocity and τ_w is the maximum wave bed shear stress. The wave friction factor f_w usually depends on the wave Reynolds number $A^2\omega/\nu$ where A is the wave orbital amplitude, ν is the kinematic viscosity, and $\omega = 2\pi/T$ is the wave frequency (T being the wave period) and on the apparent bed roughness (A/K_s with $K_s = 30\, z_0$ the apparent bed roughness) [*Jonsson*, 1966]. Many different expressions have been introduced, both explicit [e.g., *Swart*, 1974; *Kamphuis*, 1975; *Nielsen*, 1992; *Madsen*, 1994] and implicit [e.g., *Jonsson*, 1966; *Grant and Madsen*, 1979, 1986; *Styles and Glenn*, 2000].

[20] While knowledge of τ_w is sufficient for wave-only cases, the representation of the bed shear stress is more complex for wave-current cases because of the nonlinear interactions between waves and currents (Figure 3), and both the mean and the maximum combined bed shear stresses usually need to be determined. For example, maximum and mean values are used in some bed load calculations [*Soulsby and Damgaard*, 2005], and the maximum value is typically used in equation (9). A common approach has been to consider the mean current to follow a rough wall log law for which the roughness is enhanced by the presence of the wave boundary layer [e.g., *Grant and Madsen*, 1979; *Fredsøe*, 1984; *Madsen*, 1994]. The enhanced roughness is in turn a function of the stresses, which results in the need for iterative solutions. An issue for morphological coastal area models may then be the computational cost of the wave current bed shear stress calculations. *Soulsby* [1995] and *Soulsby and Clarke* [2005] provided more efficient algorithms by using explicit formulas for both the friction factor and the wave-current stresses.

[21] Another approach to the parameterization of the wave-current interactions has been provided by *Mellor* [2002] and is based on approximating the results of an intrawave model that uses a two-equation turbulence model [*Mellor and Yamada*, 1982] in combination with the law of the wall. The effect of waves on the mean flow is then accounted for by introducing an additional apparent turbulent kinetic energy production due to waves, which is a function of the wave orbital velocity, the wave period, the angle between the current and wave directions, and the bed roughness.

[22] All these approaches provide some parameterization that depends on the orbital motion in a monochromatic sense: that is, one value is used for each of the orbital velocity, period, and direction. This also extends to models considering a near-bottom orbital velocity directional spectrum for which one representative value for each of the orbital velocity, period, and direction is used [e.g., *Madsen*, 1994]. For non-

monochromatic waves, an important issue is then how the boundary layer model wave inputs (orbital velocity, period, and direction) are determined from the wave spectrum, for which several methods are available [e.g., *Soulsby*, 1987; *Madsen*, 1994; *Wiberg and Sherwood*, 2008].

3.1.3. Bottom Roughness

[23] Whether for currents, waves, or combinations of the two, the bottom shear stress determination always depends on the bed roughness, which is associated with the grain roughness, bed load sediment transport, and the presence of ripples. Roughness lengths are generally considered to be additive, and the total bed roughness has traditionally been the sum of the three roughnesses just introduced [e.g., *Grant and Madsen*, 1982; *Xu and Wright*, 1995; *Li and Amos*, 2001]. However, *Harris and Wiberg* [2001] argued that the total roughness should only be the larger of the bed load and bed form roughnesses.

[24] The equivalent grain roughness is taken to be proportional to the sediment grain diameter: $K_{sg} = 2.5 \, D_{50}$ is commonly used. The bed load roughness is related to the value of the excess Shields parameter, and several expressions have been introduced [e.g., *Grant and Madsen*, 1982; *Wiberg and Rubin*, 1989; *Xu and Wright*, 1995; *Li and Amos*, 2001].

[25] The bed form roughness is typically estimated as a function of the geometric characteristics of the bed forms [e.g., *Grant and Madsen*, 1982; *Nielsen*, 1992], which are in turn determined empirically using ripple predictors:

$$K_{sr} = a_r \frac{\eta_r^2}{\lambda_r}, \qquad (6)$$

where η_r and λ_r are the ripple height and length, and a_r is a constant taken to be $a_r = 27.7$ by *Grant and Madsen* [1982] and $a_r = 8$ by *Nielsen* [1992].

[26] There exist a number of ripple predictors, and we do not aim to present here an exhaustive list, an example of which can be found in the work by *Soulsby and Whitehouse* [2005]. Predictors usually focus on determining the ripple dimensions (η_r and λ_r) for current-generated, wave-generated, or wave-current ripples. However, many more deal with wave-only scenarios than with current-only or wave-current cases, and a large majority deal with equilibrium ripples rather than transient ripples. Current ripple dimensions are typically expressed as functions of the sediment diameter and the bed shear stress [e.g., *van Rijn*, 1993; *Soulsby*, 1997], while three main parameterization approaches can be distinguished for wave ripples. The values η_r and λ_r can be expressed as functions of the ratio of the wave orbital amplitude divided by the sediment diameter [e.g., *Wiberg and Harris*, 1994], to which another parameter may also be added: *Mogridge et al.* [1994] and *Traykovski* [2007] give functions that also contain the influence of the wave period. Another approach is to express ripple dimensions as functions of the wave mobility number $\Psi = (A\omega)^2/(s - 1)gD_{50}$ [e.g., *Nielsen*, 1981; *O'Donoghue et al.*, 2006], where s is the sediment specific gravity and g is the gravitational acceleration. Finally, the last approach relates the ripple height and ripple length to the skin-friction Shields parameter [e.g., *Grant and Madsen*, 1982]. Fewer predictors are available for wave and

current combinations. One is that of *Li and Amos* [1998], which distinguishes between five regimes (no transport, ripples in weak transport, ripples in equilibrium range, ripples in break-off range, and plane bed) and introduces subsequent regime-specific relationships based on the value of the bed shear stress.

[27] Since all predictors are empirical curve fits to field and laboratory data, they should produce similar predictions for identical given inputs. This is not the case, and significant disagreement can be observed [*Soulsby and Whitehouse*, 2005]. Unfortunately, and in spite of intercomparison studies, no predictor can be deemed unequivocally superior to the others. Nevertheless, the predictor of *Wiberg and Harris* [1994] has found wide use in large-scale models and has since been extended to wave-current cases [*Davies and Villaret*, 2000] and expressed in an noniterative manner [*Malarkey and Davies*, 2003].

[28] Finally, such a sum of grain, bed load, and bed form roughnesses leads to the total bed shear stress. However, in sediment transport modeling, the skin friction stress is crucial and thus needs to be estimated. One approach that can be used in coastal area models relates the skin friction stress (τ_{sf}) to the maximum wave-current bed shear stress (τ_{wc}) and the bed form dimensions [*Smith and McLean*, 1977; *Wiberg and Nelson*, 1992]:

$$\tau_{sf} = \tau_{wc} \left[1 + \frac{C_d}{2\kappa^2} \frac{\eta_r}{\lambda_r} \left(\ln \frac{30\eta_r}{K_{s,sf}} - 1 \right)^2 \right]^{-1}, \qquad (7)$$

where $C_d = 0.5$ [*Smith and McLean*, 1977] and $K_{s,sf}$ represents the hydraulic roughness of the bed surface, consisting of the grain and bed load roughnesses.

3.2. Bed Load Sediment Transport

[29] Bed load is often linked to migration of bed features. It is the part of sediment transport that is due to interparticle interactions and which occurs in a thin near-bed region of high sediment concentration (Figure 2). As such, it cannot be resolved by coastal multidimensional models for which sediment is implicitly assumed to be dilute, and it is instead described by relating the bed load transport rate to the bottom shear stress. Such relationships have now been investigated both empirically and theoretically for several decades, and a number of different formulations exist.

[30] The bed load transport rate has been measured directly in many experimental studies using bed load traps, leading to empirical formulas for steady uniform flow [e.g., *Meyer-Peter and Müller*, 1948; *Wilson*, 1966] and, more recently, for wave-current flows [e.g., *Ribberink*, 1998]. Several studies also proceeded to provide theoretical and semiempirical relationships for the bed load transport rate [e.g., *Einstein*, 1950; *Bagnold*, 1966; *Bailard*, 1981; *Engelund and Fredsøe*, 1976; *van Rijn*, 1984b]. Even though this leads to a number of different expressions, many formulas reduce to relating the transport rate to a power of the excess bed shear stress with respect to the critical stress for initiation of motion:

$$\Phi_B = m\theta^n(\theta - \theta_{cr})^p, \qquad (8)$$

TABLE 1. Coefficients in Bed Load Predictors

Predictor	m	n	p
Meyer-Peter and Müller [1948]	8	0	1.5
Wilson [1966]	12	1.5	0
Fernandez Luque and van Beek [1976]	5.7	0	1.5
Ribberink [1998]	11	0	1.65
Soulsby and Damgaard [2005]	12	0.5	1
Kleinhans and Grasmeijer [2006]	1	0	1.5

where m, n, and p are constants, examples of which are given in Table 1; θ is the nondimensional bed shear stress (Shields parameter), θ_{cr} is the critical Shields parameter for initiation of motion, and Φ_B is the nondimensional bed load transport rate. While there seems to be some consensus on the powers to be used, $n + p \approx 1.5$, the values for m are more varied (Table 1). *Soulsby and Damgaard* [2005] also provided relationships for the net bed load transport in wave-current combinations by numerical integration of a power law for the time-dependent transport rate and expressed the results in terms of the bed shear stress amplitude, mean and asymmetry.

[31] Since bed load occurs very close to the bed, it is affected by the local slope of the bed, as is the critical Shields parameter. Accounting for the extra gravity term when considering driving and stabilizing forces on particles, the critical bed shear stress is reduced in presence of transverse slopes and is either reduced or increased for a longitudinal slope [*Fredsøe and Deigaard*, 1992]. For mild slopes and beds elevating in the flow direction, such a correction of the threshold is sufficient. However, for steep negative slopes an extra correction is required [*Damgaard et al.*, 1997]. For transverse slopes, the bed load direction differs from that of the flow, which leads to a lateral component that depends on the slope and the ratio of the streamwise stress over the critical bed shear stress [e.g., *Ikeda*, 1982; *Sekine and Parker*, 1992].

3.3. Erosion and Deposition of Suspended Sediment

[32] The net bottom boundary sediment flux is commonly divided into an upward part, erosion E that represents the exchange of sediment from the bed to the flow, and a downward part due to gravitational settling, deposition D (Figure 2). Several methods have been used to express erosion in terms of flow and sediment parameters, and the two most common approaches have also been closely linked to the sediment cohesiveness. For noncohesive sediment, the most widely used method has been to assume that the disequilibrium introduced by the unsteadiness remains mild and to consider the erosion flux to be equal to the entrainment rate under equilibrium conditions [*Garcia and Parker*, 1991] and thus to relate it to the reference concentration value through the settling velocity, that is, $E = c_{\mathrm{ref}}W_s$ [e.g., *Harris and Wiberg*, 2001; *Wai et al.*, 2004; *Lesser et al.*, 2004]. To ensure that the net vertical flux is not identically zero the deposition is then calculated using the nonequilibrium concentration $D = c_bW_s$, where c_b is the actual bottom concentration. For cohesive sediments, the approach of choice has been to provide a formula directly relating the

erosion flux to the flow and sediment parameters [*Blumberg*, 2002; *Lumborg and Windelin*, 2003]. This second approach has also recently been extended to study noncohesive sediment [*Warner et al.*, 2008].

[33] Such a direct parameterization has been one of the most studied issues in fine sediment transport through theoretical work, laboratory studies, and field observations. The general consensus is that bottom shear stresses are the dominant forces causing erosion while the sediment bed characteristics control the resistance to erosion. Mathematically, two formulations (a power law and an exponential law) have been introduced to relate the erosion to the bed shear stress τ_b. Usually, an excess shear stress $(\tau_b - \tau_{ce})$ is employed, where τ_{ce} represents the critical stress for erosion which is not necessarily equal to the critical stress for initiation of motion, first determined by *Shields* [1936]. The power law is often reduced to a linear expression (Figure 4) [e.g., *Ariathurai and Krone*, 1976; *Mehta et al.*, 1989; *Sanford and Halka*, 1993; *Mei et al.*, 1997] and has been used for unlimited erosion. The exponential form has instead mostly been used for depth-limited erosion with $\tau_{ce} = \tau_{ce}(z)$. However, *Sanford and Maa* [2001] recently showed that a linear erosion formula (Figure 4) may be used to represent both depth-limited and unlimited erosion, provided that both the critical bottom shear stress and the constant of proportionality increase with depth. The resulting formula can be expressed as

$$E = \rho_s(1 - p_c(z))E_0\left(\frac{\tau_b}{\tau_{ce}(z)} - 1\right), \qquad (9)$$

where p_c is the bed porosity and E_0 is a local constant. Consolidation and physico-chemical effects result in an increase of the critical stress for erosion τ_{ce} [*Winterwerp and van Kesteren*, 2004] and a decrease of the bed porosity. In turn, both depth dependencies limit the extent of erosion. These are important differences between cohesive sediments and noncohesive sediments and are often one of the main conceptual limitations (through omission) in models. For noncohesive sediments, no dependence on z is included. In spite of its wide use, this last formula does not consider all physical erosion processes. It aims to represent erosion of individual flocs or particles. However, it does not describe entrainment of fluid mud, which occurs when mud behaves as a viscous fluid; surface erosion, for which large layers of sediment are eroded; or mass erosion, when local failure within the bed results in lumps of sediment being eroded [e.g., *Winterwerp and van Kesteren*, 2004].

[34] For fine particles, deposition has commonly followed the parameterization of *Krone* [1962], which states that no deposition occurs for bed shear stresses higher than a critical shear stress for deposition τ_{cd}. Since τ_{ce} is typically taken to be greater than τ_{cd}, this implies that erosion and deposition are mutually exclusive and defines three regimes: a depositional state, for which only deposition occurs $(\tau_b < \tau_{cd})$; a stable state, for which neither erosion nor deposition occur $(\tau_{cd} < \tau_b < \tau_{ce})$; and an erosional state for which only erosion occurs $(\tau_{ce} < \tau_b)$ [e.g., *Li and Amos*, 2001]. For noncohesive sediments, no deposition critical stress is usually employed and deposition and erosion are not mutually

$$\frac{dm}{dt} = 0.002\,(\tau_0 - \tau_e)\ \text{(SI units)}$$
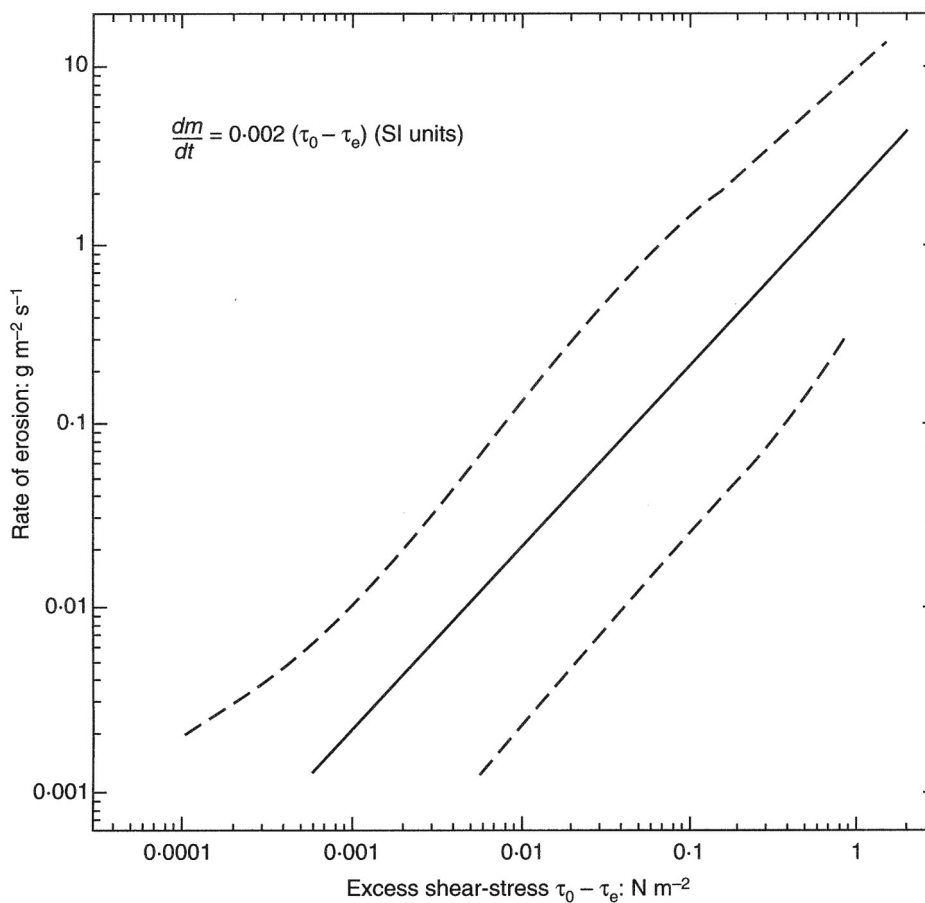
Figure 4. Erosion rate for cohesive sediment in currents as a function of excess shear stress. The dashed lines indicate the limits of scatter in experimental data [after *Delo*, 1988].

exclusive. This paradigm of mutual exclusion for cohesive sediments has now been challenged. *Sanford and Halka* [1993] assessed it using model-data comparisons of deposition in the upper Chesapeake Bay and concluded that mutually exclusive erosion and deposition fail to explain many field observations. Additionally, *Winterwerp and van Kesteren* [2004] argue that this paradigm of mutually exclusive deposition and erosion is not supported by a sound explanation of the physical processes involved.

3.4. Sediment Diffusivity

[35] Sediment diffusivity specifications are typically split between horizontal diffusion K_h and vertical diffusion K_v. Horizontal diffusion is commonly neglected, taken to be constant, or based on simple formulations [e.g., *Smagorinsky et al.*, 1965]. In contrast, the vertical diffusion uses a more advanced closure, which is closely linked to the flow turbulence closure. K_v is related to the eddy viscosity ν_t through a Schmidt number σ_s:

$$K_v = \frac{\nu_t}{\sigma_s}. \tag{10}$$

The turbulent diffusivity is usually larger than the eddy viscosity because of centrifugal forces in turbulent eddies ejecting particles to the outside of eddies, which results in

Schmidt numbers being typically less than one. A relatively common approach is to assume that the sediment Schmidt number is equal to the Prandtl number used for heat and buoyancy.

[36] Such an approximation does not effectively consider a possible dependence of σ_s on sediment parameters, in spite of results from a number of studies. *Van Rijn* [1984a] related the sediment turbulent diffusivity to the turbulent eddy viscosity through two parameters:

$$K_v = \beta\phi\nu_t. \tag{11}$$

The first, called β, was found to be a function of the settling velocity and the bed friction velocity and can be seen as expressing the relative importance of the particles' gravitational inertia with respect to the flow turbulence. The other is a function of the concentration and represents the effect that the presence of particles has on the sediment diffusivity (i.e., suppressing turbulence). Several other studies have followed and considered β. This parameter was found to exhibit a dependence on the grain diameter [*Hill et al.*, 1988; *Villatoro et al.*, 2010]. However, it also depends on the turbulent characteristics of the flow, and several different mathematical formulas that are based on the ratio of settling velocity over friction velocity have been introduced [e.g.,
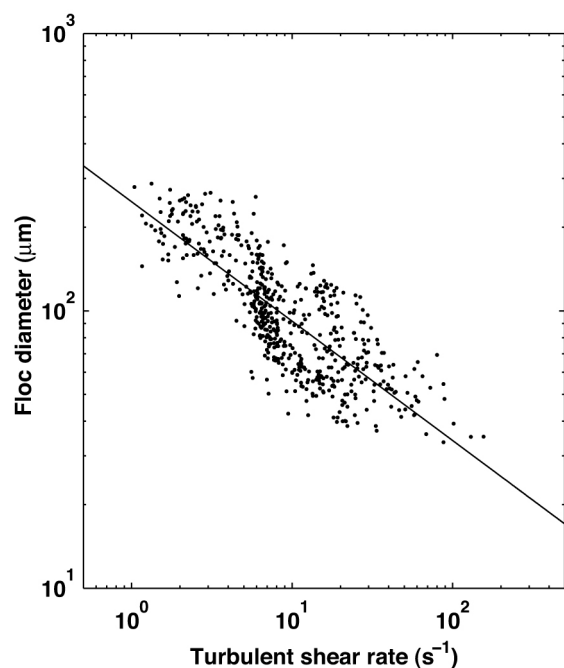
Figure 5. Floc size as a function of turbulent shear rate (G) in the Dee Estuary, United Kingdom.

Hill et al., 1988; *Whitehouse*, 1995; *Rose and Thorne*, 2001; *Graf and Cellino*, 2002]. Fewer studies have pursued a concentration dependence [e.g., *Amoudry et al.*, 2005]. Finally, experimental process studies can now provide vertical profiles of sediment diffusivity [e.g., *Graf and Cellino*, 2002; *Thorne et al.*, 2009], which may then be used to develop and assess appropriate parameterizations.

3.5. Settling Velocity

[37] The sediment settling velocity W_s is an important parameter both in the determination of the suspended concentration profile and in the near-bed conditions, and it depends on the sediment and flow parameters. Some common approaches in coastal area models are to set it either as a user-specified, sediment-specific parameter or to employ formulas relating it to sediment and flow parameters. It has also been observed that the settling of sediment depends on the local concentration. This relationship is traditionally taken to follow the experimental results of *Richardson and Zaki* [1954] for noncohesive sediments:

$$W_s = W_{s0}(1 - k_1 c)^{n_1}, \tag{12}$$

where W_{s0} is a reference settling velocity, k_1 is a constant, and n_1 depends on the particle Reynolds number varying from 2 to 5.

[38] For cohesive sediments, a common formulation is that of *Mehta* [1986], which gives

$$W_s = k_2 c^{n_2} \tag{13}$$

for moderate concentrations and an expression of the type of equation (12) at higher concentrations. The k constants depend on the sediment composition, and n_2 varies from 1 to

2 while $n_1 \approx 5$ for cohesive sediments. However, the *Mehta* [1986] expression only relates the settling velocity of cohesive sediments to the suspended sediment concentration and does not really account for the influence of flocculation on W_s. Following recent work on turbulence-induced flocculation, *Winterwerp* [2002] introduced a formula expressing hindered settling of suspended cohesive sediments as a function of both the suspended sediment concentration and the concentration of flocs, and *Winterwerp et al.* [2006] expressed the settling velocity as a function of the suspended sediment concentration and the local shear stress.

3.6. Cohesive Sediments

[39] Suspended cohesive sediment concentration is determined by a combination of processes more complicated than those accounted for so far, such as flocculation, consolidation, and liquefaction. Flocculation is the formation and break up of flocs of cohesive sediment and is a key process in differentiating cohesive and noncohesive sediments. Consolidation and liquefaction are processes by which the bed is either strengthened or weakened. In addition, settling, the interaction between particles and turbulence, deposition, and erosion are typically modeled differently for cohesive and noncohesive sediments. However, these processes are not specific to cohesive sediments and were discussed in sections 3.3, 3.4, and 3.5. Presently, most cohesive sediment models that do account for processes such as flocculation and consolidation are implemented in one dimension [e.g., *Winterwerp*, 2002; *Neumeier et al.*, 2008; *Sanford*, 2008]. In most multidimensional models, cohesive sediments are modeled in simpler ways, and, in general, only cohesive-specific formulations for settling, deposition, and erosion are considered, while both flocculation and consolidation are neglected.

[40] In flocculation models, mud flocs are commonly treated as self-similar fractal entities [*Kranenburg*, 1994; *Winterwerp and van Kesteren*, 2004], and fractal theory is employed to derive equations for the floc's properties (size, settling velocity, density, and strength). *Winterwerp* [2002] derived balance equations for both the floc size and for the number of mud flocs in the turbulent fluid, which can be viewed as advection-diffusion equations with an extra nonlinear term due to the aggregation and floc breakup processes [*Winterwerp and van Kesteren*, 2004]. However, the main issue for multidimensional models is really how to parameterize the effect of flocculation on the floc size, density, and settling velocity without resolving the flocculation processes per se. For example, *Neumeier et al.* [2008] use a set of equations directly relating the floc length scale, effective diameter, and median settling velocity to the suspended sediment concentration following *Whitehouse et al.* [2000]. This issue is similar to that encountered in bed load modeling, and the importance of empirical studies should be relatively evident. These usually seek to relate the floc's properties to some parameterization of the turbulent cohesive suspension (Figure 5), and common quantities used are the suspended sediment concentration and the shear rate at the smallest turbulence length scale $G \equiv \sqrt{\varepsilon/\nu}$, where G
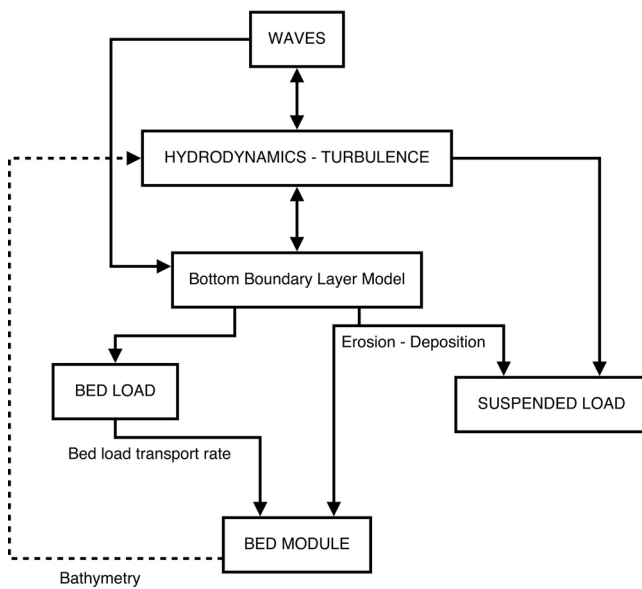
Figure 6. General structure of sediment transport models in coastal ocean models.

is the shear rate at the smallest turbulence scale which is the inverse of the Kolmogorov scale, ε is the turbulence dissipation rate, and ν is the kinematic viscosity [e.g., *Lick et al.*, 1993; *Dyer and Manning*, 1999; *Manning and Dyer*, 1999]. The derived empirical expressions usually relate the floc diameter to both the concentration and G and relate the floc settling velocity to the floc size. *Winterwerp et al.* [2006] used the *Winterwerp* [2002] model to derive semiempirical expressions for the floc size and settling velocity, which are calibrated by field experiments. Unfortunately, such expressions are generally not nondimensional and involve determination of empirical dimensional constants.

[41] Self-weight consolidation is the consolidation of cohesive sediment deposits under the influence of their own weight. When flocs settle and accumulate on the bed, they are squeezed by the flocs settling on top of them. Pore water is then driven out of the intrafloc and interfloc spaces. This process can result in large vertical deformations of the bed. Consolidation is commonly described by the Gibson equation [*Gibson et al.*, 1967], which is a one-dimensional equation for the void ratio.

4. COASTAL AREA SEDIMENT TRANSPORT MODELING

4.1. Implementation of Physical Processes in Coastal Area Models and Morphological Updating

[42] The approaches described above are usually implemented within systems that combine hydrodynamic models, turbulence models, and wave models. Turbulence models in regional models typically use a Reynolds-averaged Navier-Stokes (RANS) approach and will be discussed in more detail in section 5.3. An increasingly popular option seems to be to couple the hydrodynamic model to a turbulence model able to implement a variety of RANS closures (e.g., the General Ocean Turbulence Model; see www.gotm.net). Waves are

often modeled through coupling to an external model, such as the Simulating Waves Nearshore (SWAN) model [*Booij et al.*, 1999] or the Wave Model [*Komen et al.*, 1994]. The general structure of sediment transport modules in these systems can be illustrated by Figure 6. The interconnected hydrodynamics, turbulence, and wave models provide the necessary inputs. The bottom boundary layer methods reviewed in section 3.1 are then implemented to obtain the bed shear stress. In turn, τ_b is used to calculate the sediment exchange between the bed and the flow (erosion and deposition, section 3.3) and the bed load transport rate (section 3.2). Finally, the suspended sediment and bed module solve the governing equations introduced in section 2.1 and may incorporate cohesive processes. The output of the bed module, that is, the bathymetry, is then taken into account in the hydrodynamic computations.

[43] The location of the seabed is usually updated dynamically through a mass conservation concept (equation (3)). When fully coupled with the hydrodynamic model, this process may calculate at each time step the mass change incurred from erosion, deposition, and horizontal flux divergence. Such mass change is then translated into a bed level change. An important issue then arises from the time-scale difference between morphological evolution (on the order of weeks to years) and the hydrodynamic flow time scale (hours for tidal flows). One technique often used to improve the efficiency of morphological predictions is to introduce a morphological acceleration factor to speed up morphological change. The crucial concept is that the hydrodynamics should not be influenced and the implementation usually simply multiplies the different components of the bed mass balance. The validity of this approach then relies on both large differences in time scales between hydrodynamics and bed changes and on a linear response of morphology to external forcing. *Jones et al.* [2007] assessed the reliability of the morphological acceleration factor method in terms of stability and adherence to linearity. Stability was severely limited for factors above 25, and nonlinear responses were found to start for morphological factor values decreasing with increasing strength of forcing. Other issues with the method may also appear. The order of events in tidal cycles may change, leading to conflicts with sediment availability and bed stratigraphy [*Delft Hydraulics*, 2007]. Spring-neap tidal variability may also result in locally increased or decreased bed changes at the time scale of the spring-neap cycle multiplied by the morphological factor, and this approach should be used with caution.

4.2. Coastal Area Sediment Transport Numerical Models

[44] Numerous models of varying complexity aim to describe sediment processes in coastal regions following the approaches presented in the previous sections. We will only review here in detail five widely used area models that can provide some insight on the suspended sediment concentration and track two-dimensional bed changes. Both 2DH models (e.g., x-y), which solve depth-averaged equations, and fully three-dimensional models (e.g., x-y-z, with z as the vertical coordinate) may satisfy this requirement. However,

TABLE 2. Coastal Morphological Sediment Transport Models

Model	Model Type	Mesh[a]	Source[b]
ROMS	3-D	FD	OS, LD
Delft3D	3-D	FD	C[c]
ECOMSED	3-D	FD	OS, LD
TELEMAC	2-DH	FE	OS, LD
MIKE	quasi 3-D	FV	C

[a]FD, finite difference; FE, finite element; and FV, finite volume.
[b]OS, open source; LD, limited distribution; and C, commercial.
[c]Delft3D flow, morphology, and wave modules are now available via open source.

2DV models (e.g., x-z) [e.g., *Rakha et al.*, 1997; *Zhang et al.*, 1999; *Harris and Wiberg*, 2001; *Hsu et al.*, 2006] only calculate one-dimensional bathymetric evolutions and are therefore excluded, even though they are commonly based on the same parameterizations as those discussed in section 3. Other three-dimensional models are excluded because they fail to track morphodynamic changes [e.g., *Burchard et al.*, 2004; *Pandoe and Edge*, 2004].

[45] The five models discussed hereafter are (1) the U.S. Community Sediment Transport Model (CSTM), which is embedded in the Regional Ocean Model System (ROMS) [*Warner et al.*, 2008] (as well as in the Finite Volume Coastal Ocean Model (FVCOM) and recently in the Proudman Oceanographic Laboratory Coastal Ocean Modeling System); (2) the Delft3D modeling system [*Lesser et al.*, 2004; *Delft Hydraulics*, 2007]; (3) the Estuarine Coastal Ocean Model with Sediment Transport (ECOMSED) model [*Blumberg*, 2002]; (4) the sediment transport model (SISYPHE) coupled with TELEMAC [*Villaret*, 2004], and (5) the MIKE modeling system [*DHI*, 2004, 2006, 2007a, 2007b]. All these models can also be coupled to a wave model and obtain the bed shear stress using diverse methods for wave-current interactions. A summary of some characteristics of these models are given in Tables 2 and 3, and further details on each model are presented in sections 4.2.1–4.2.5. Table 2 focuses on model characteristics (number of dimensions resolved, discretization method, and code availability), while Table 3 focuses on which sediment processes are implemented in the model. Wave-current interactions, sediment erosion, and deposition are not mentioned as all models account for such processes, albeit via different parameterizations.

4.2.1. CSTM-ROMS

[46] This three-dimensional model [*Warner et al.*, 2008] implements sediment algorithms for an unlimited number of noncohesive sediment classes and for the evolution of the bed morphology within the finite difference coastal circulation model ROMS [*Haidvogel et al.*, 2008]. The model also provides two-way coupling between ROMS and the wave model SWAN and a turbulence model using the generalized length-scale method of *Umlauf and Burchard* [2003]. Bottom boundary parameterizations range from simple drag coefficient expressions (linear, quadratic, and logarithmic profile) to formulations representing wave-current interactions [e.g., *Madsen*, 1994; *Soulsby*, 1995; *Styles and Glenn*, 2000, 2002]. Suspended sediment concentration is computed with the same advection-diffusion

algorithms as for other tracers. The sediment bed is represented by a multilayer structure that allows tracking of layer porosity, mass, and thickness. The exchange between the hydrodynamic flow region and the bed is prescribed using flux formulations for erosion and deposition between the flow and the top layer of the bed. In particular, the erosion depends linearly on the bed shear stress and is limited by the amount of sediment in the active layer. Bed load transport is included and can be calculated following the *Meyer-Peter and Müller* [1948] formula for unidirectional flow or following the *Soulsby and Damgaard* [2005] formulation for combined waves and currents, both of which are modified to account for bed slope effects.

4.2.2. Delft3D

[47] The sediment module in Delft3D [*Lesser et al.*, 2000, 2004; *Delft Hydraulics*, 2007] implements algorithms for up to five different classes within a three-dimensional hydrostatic free-surface flow solver. Suspended sediment concentration is obtained from an advection-diffusion equation, and exchange between the bed and the flow depends on the sediment type (mud or sand). For muds, the exchange term is always added to the bottom grids and is computed using a linear equation for erosion and the Krone deposition formula [*Krone*, 1962]. For sands, the reference concentration approach is employed in which (1) a reference height and the corresponding reference concentration are calculated [*van Rijn*, 1984a] and (2) sediment exchange is located in the first cell entirely above the reference elevation (reference cell) and calculated assuming a linear gradient between the reference concentration and the concentration in the reference cell. The bed load transport rate is calculated following expressions that are based on the *van Rijn* [1984b] and *van Rijn* [1993] formulas, and the effects of the bed slope are included. The bed shear stress is given by the formulation of *van Rijn* [1993]. Morphological change uses a correction due to suspended load transport under the reference level and a morphological factor that allows acceleration of morphological changes.

4.2.3. ECOMSED

[48] ECOMSED [*Blumberg*, 2002] only implements two sediment classes, one noncohesive and one cohesive, in a three-dimensional, time-dependent coastal ocean circulation model based on the Princeton Ocean Model [*Blumberg and Mellor*, 1987]. The suspended sediment concentration is calculated by solving the advection-diffusion equation. For

TABLE 3. Modeled Processes in the Coastal Morphological Models

Model	SIS[a]	Sediment Mixtures	Bed Load	K_v	W_s	Cohesive Sediment
ROMS	yes	yes	yes	$\sigma_s = Pr$[b]	constant	no
Delft3D	yes	yes	yes	$K_v = \beta \nu_t$	$W_s = f(S, c)$[c]	yes
ECOMSED	no	no	no	$\sigma_s = Pr$[b]	$W_s = f(c)$	yes
TELEMAC	no	yes	yes[d]	-	constant	yes
MIKE	yes	yes	yes[d]	-	$W_s = f(c)$	yes

[a]SIS is sediment-induced stratification.
[b]Pr is the buoyancy Prandtl number.
[c]S is the salinity.
[d]Not necessarily separated from total load depending on formulation used.

cohesive sediments, the erosion is modeled as a power of the excess bed shear stress and the deposition is modeled following the formula of *Krone* [1962]. The settling velocity is taken to be a function of concentration and velocity shear following *Burban et al.* [1990]. For noncohesive sediments, the erosion is modeled following a reference concentration approach [*van Rijn*, 1984a] to which a coefficient representing bed armoring is applied, while deposition is due to the self-weight of the grains. The sediment bed is segmented into seven layers, the thicknesses of which are calculated from mass conservation. Erosion and deposition only occur in the topmost layer, and bed load is not considered. Instead, the suspended load transport is calculated from the reference concentration following the procedure from *van Rijn* [1984a]. The bottom shear stress is calculated using a logarithmic profile approach for currents only and using the *Grant and Madsen* [1979] wave-current model otherwise.

4.2.4.   TELEMAC and SISYPHE

[49]   The TELEMAC finite element system includes a three-dimensional hydrodynamic module (TELEMAC-3D) and a two-dimensional module (TELEMAC-2D) which solves the depth-averaged Saint-Venant equations. Both models can be internally coupled to the two-dimensional sediment transport and morphodynamic model (SISYPHE) [*Villaret*, 2004]. For two-dimensional coupling, the total bed shear stress, depth-averaged velocity field, and water depth is sent to the morphodynamic model at each time step, which sends back the bed evolution. A wave module (TELEMAC-based Operational Model Addressing Wave Action Computation (TOMAWAC)) also exists but is not automatically fully coupled to the hydrodynamic and sediment transport components [*Brown and Davies*, 2009]. Sand transport, divided into a bed load and a suspended load, is computed for up to 10 different sediment classes, and several options are available at most stages. For bed load, sand transport rate can be calculated from a choice of formulations, such as *Meyer-Peter and Müller* [1948], *Einstein* [1950], and *Engelund and Hansen* [1967] for currents only and *Bijker* [1969], Soulsby–van Rijn [*Soulsby*, 1997], *Bailard* [1981], and *Dibajnia and Wanatabe* [1992] for combined waves and currents. Bed slope effects and a hiding exposure factor are also considered. The suspended sediment concentration is obtained by solving a depth-averaged advection-diffusion equation, and the exchange between the bed and the suspended load (erosion and deposition) is modeled using either a linear erosion and deposition following *Krone* [1962] or the net upward flux following *Celik and Rodi* [1988] with the *Zyserman and Fredsøe* [1994] reference concentration. The suspended sediment concentration can also be calculated by solving a 3-D transport equation within TELEMAC-3D. In the 2-D suspended sediment transport models, the convection velocity can be corrected in order to account for sediment concentration and velocity distributions in the vertical.

[50]   SISYPHE can also be used alone, and the hydrodynamics are then read from a previous hydrodynamic results file. In this case, the bed shear stress is related quadratically to the depth-averaged current in the absence of waves with a

choice between using the Chézy coefficient, the Stickler coefficient, the Manning coefficient, or a log law. A correction factor is applied for skin friction, where the skin roughness can be related to the sand grain diameter or to the ripple height, according to the *van Rijn* [2001] procedure. For pure waves, the *Swart* [1974] friction factor is used, and a wave-current friction factor is calculated from the current-only stress, the wave-only stress, the depth-averaged current, and the wave-orbital velocity [*Villaret*, 2004].

4.2.5.   MIKE

[51]   MIKE21 FM is a cell-centered finite volume model with an unstructured (flexible) mesh in the horizontal and a quasi 3-D description over the vertical that contains several modules. MIKE21 SW [*DHI*, 2004] is a directional spectral wave model describing the wavefield including refraction, wave breaking, bed friction, wind forcing, and an approximate representation of diffraction. The flow module MIKE21 HD [*DHI*, 2006] solves the Saint-Venant equations. It can be coupled with MIKE21 SW to include driving forcing from wave breaking, current refraction, and flow resistance taking wave-current boundary layer interaction into account [*Fredsøe*, 1984]. The mud transport module, MIKE21 MT [*DHI*, 2007a], represents advection-dispersion, sedimentation with a concentration-dependent settling velocity, and erosion. For cohesive sediment a multilayered bed structure can be invoked. The transport of sand under combined waves and current model, MIKE21 ST [*DHI*, 2007a], is based on a model for the vertical distribution of the turbulence with interaction between the wave and current boundary layers [*Fredsøe*, 1984] and turbulence generated by wave breaking [*Deigaard et al.*, 1986]. The sediment transport is divided into bed and suspended load with bed boundary conditions from *Engelund and Fredsøe* [1976]. The instantaneous suspended sediment concentration profile is found by a quasi 3-D approach which solves the vertical diffusion equation on an intrawave-period basis [*Fredsøe et al.*, 1985]. The suspended sediment transport in the mean current direction and normal to it is found by vertical and time integration of the product of instantaneous current and concentration profiles. A morphological module allows for simulation of the temporal development in the bathymetry.

5.   DISCUSSION

5.1.   Assessment of Coastal Modeling Approaches

[52]   Several shortcomings relating to the models presented can be quickly inferred from Tables 2 and 3. The most advanced model would be fully three-dimensional, would use unstructured meshes (i.e., finite volume approach), and would include all processes in Table 3. No model achieves all. Further discussion on specific modeling approaches and issues is presented in sections 5.1.1–5.1.6. However, we refrain from general recommendations because of the inherent dependence on specific applications and users.

5.1.1.   Buoyancy Stratification

[53]   As mentioned previously, not all models solve the full three-dimensional equations of motion. In particular, MIKE uses a quasi 3-D approach and SISYPHE uses a 2-DH
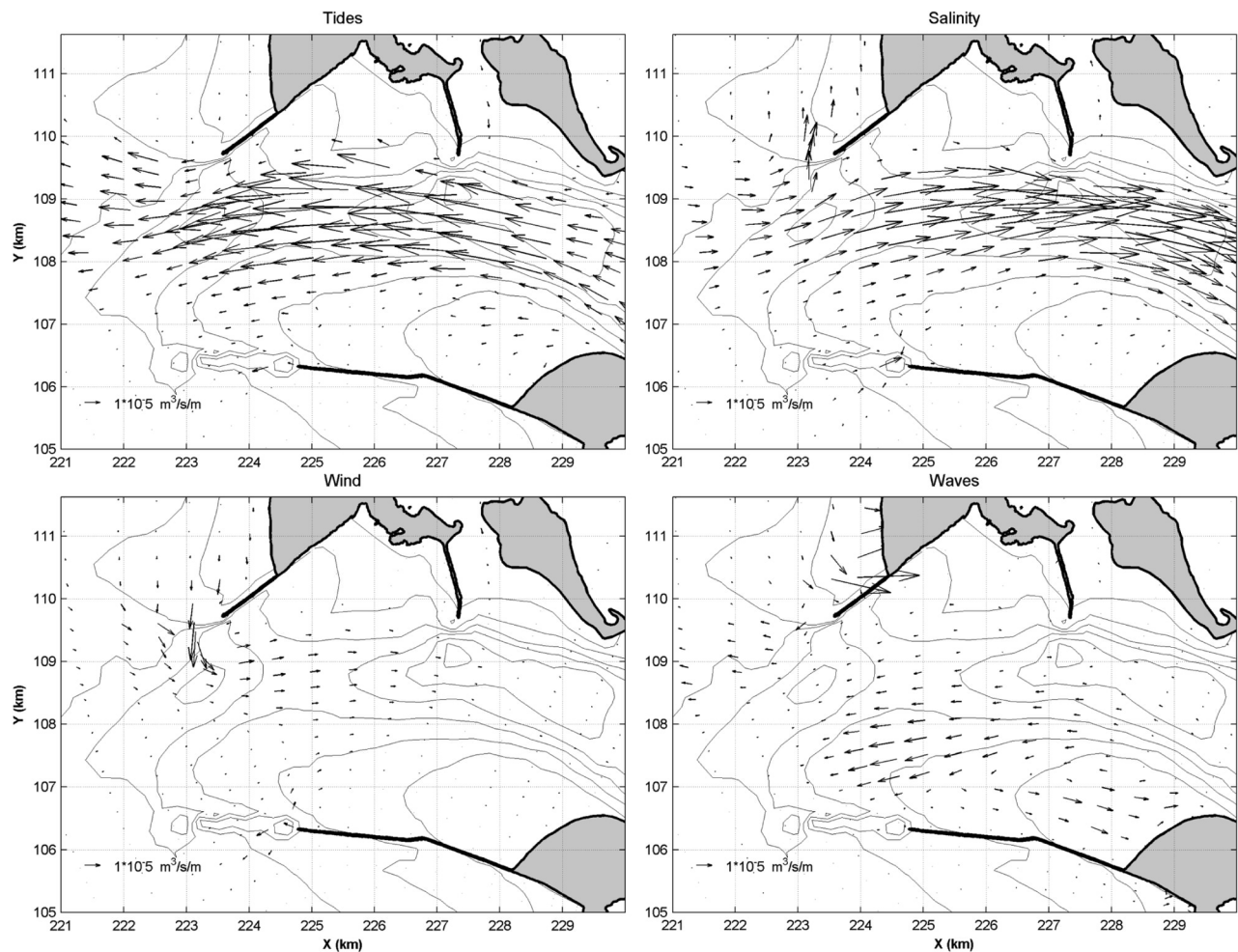
Figure 7. Effect of salinity stratification on sediment transport [after *Elias and Gelfenbaum*, 2009]. (top left) Sediment transport at the mouth of the Columbia River for a nonstratified case due to tides and saline river inflow, (top right) salinity-driven sediment transport for a stratified case with fresh river inflow, and separate contributions of (bottom left) wind and (bottom right) waves to the transport rates.

approach. Although two-dimensional approaches may yield satisfactory results for unstratified flows, 2-DH models are unable to represent baroclinic behaviors that can be of importance in coastal environments and estuaries. For example, *Pandoe and Edge* [2004] showed very different suspended sediment responses to barotropic and baroclinic modes in the idealized case of a barred rectangular basin. *Burchard et al.* [2008] also discussed how density differences significantly contribute to the net suspended sediment accumulation in the Wadden Sea. Finally, *Elias and Gelfenbaum* [2009] assessed which physical processes are responsible for sediment transport at the mouth of the Columbia River and found that sediment transport, when accounting for density stratification, is near-equal but opposite directed to the nonstratified case (Figure 7).

5.1.2. Grid Discretization

[54] Another crucial issue concerns the discretization method employed. Most models use a finite difference approach, but a growing number of coastal hydrodynamic models employ unstructured grids and finite elements or finite volume approaches. Such approaches provide inter-

esting geometric flexibility that tolerates local grid refinement and allows better fits to irregular coastlines. *Chen et al.* [2003, 2007] recently showed that the finite volume method is indeed superior to finite differences in terms of accuracy in cases of complex coastal geometry and steep bottom slope (Figure 8).

5.1.3. Sediment-Induced Stratification

[55] Not accounting for the effects of the sediment on density (equation (1)) amounts to neglecting the sediment-induced stratification of the flow. These sediment-buoyancy effects are crucial in coastal area models, enabling them to represent the turbulence damping due to the presence of suspended sediment [e.g., *Villaret and Trowbridge*, 1991; *Winterwerp*, 2001]. Including these effects also leads to a reduction of the bed stress, which has been observed for sediment-laden flows [e.g., *Thompson et al.*, 2006]. In addition to better physical representation, sediment-induced stratification can lead to nonnegligible effects on sediment dynamics in tidally dominated coastal environments [*Byun and Wang*, 2005], and the damping of turbulence by sediment buoyancy has also been found to contribute signifi-
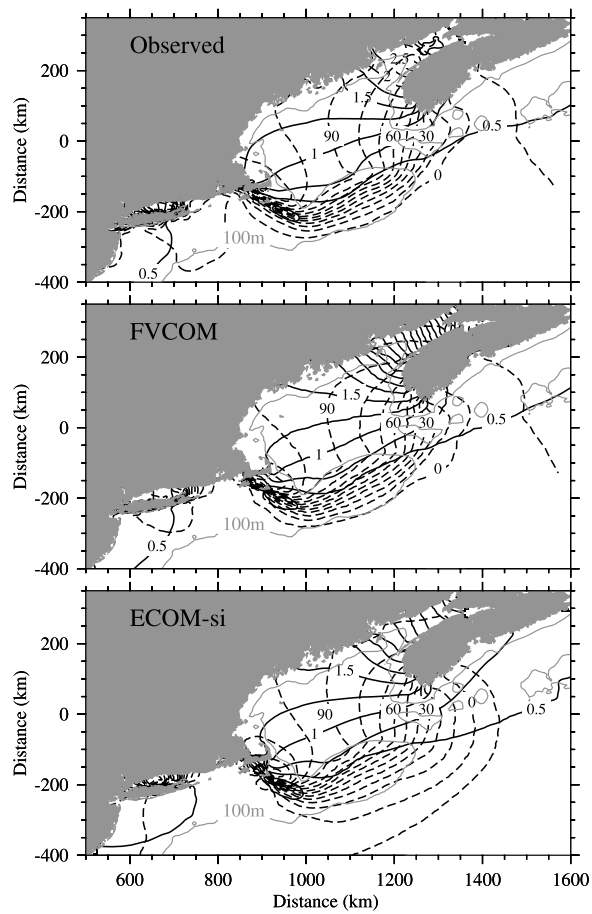
Figure 8. (top) Comparison between observation, (middle) finite-volume predictions using FVCOM, and (bottom) finite difference predictions using ECOM-si for the M_2 tidal amplitudes and phases in the Gulf of Maine and Georges Bank region [after *Chen et al.*, 2007].

cantly to the turbulent kinetic energy balance [*Safak et al.*, 2010].

5.1.4. Bed Load Modeling

[56] In general, several bed load formulations are implemented in coastal area sediment models. Independently from the quality of the bed load predictions, it is important to consider the restrictions associated with given approaches. Many of the formulations implemented are restricted to bed load transport by currents only [*Meyer-Peter and Müller*, 1948; *Einstein*, 1950; *Engelund and Hansen*, 1967; *Engelund and Fredsøe*, 1976; *van Rijn*, 1984b]. The *Bijker* [1969] expression does consider a wave-current bed shear stress but always leads to sediment transport in the direction of the current. Finally, even the formulations that do consider bed load transport under waves and currents superimposed at an angle [e.g., *Dibajnia and Wanatabe*, 1992; *Soulsby*, 1997; *Soulsby and Damgaard*, 2005] still make simplifying assumptions, on the shape of the waves for example. In addition to such flow-related restrictions, bed load empirical formulas are characterized by some nonnegligible uncertainty and are often only deemed accurate within a factor of 5–10. The use of bed load traps introduces some errors due to flow modification induced by the trap and the difficulty in distinguishing the bed load and the suspended load in trapped sediment. Most formulas have also been derived for sediments of diameters larger than 200–300 μm, which raises the issue of validity for finer particles.

5.1.5. Flow-Bed Exchange Rate

[57] As mentioned in section 3.3, the exchange between bed and suspension is generally modeled differently for mud and for sand. Most of the models reviewed use a cohesive erosion that follows a power or exponential form and a cohesive deposition that follows *Krone* [1962], the pertinence of which we already discussed in section 3.3. These models then use a reference concentration approach for noncohesive sediments. The notable exception to this general modeling approach is the U.S. Community Sediment Transport Model implemented in ROMS, in which noncohesive sediments are eroded following an expression similar to equation (9). The obvious advantage is the simplicity and the flexibility of such a formulation to accommodate the erosion of both cohesive and noncohesive sediments. The issue is then whether such a linear relationship between erosion and bed shear stress is appropriate for noncohesive sediments. While this form is undoubtedly different from the more typical formulations used in the reference concentration approach [see, e.g., *Garcia and Parker*, 1991], linear expressions for the reference concentration have previously been introduced [e.g., *van Rijn*, 1993]. They may be considered as an approximation to more typical expressions, and they have been found to give satisfactory results in a one-dimensional intrawave two-phase dilute model [*Amoudry et al.*, 2005].

5.1.6. Cohesive Sediments

[58] Only the sediment transport model in ROMS does not treat cohesive sediments explicitly. Most of the remaining models only account for cohesive sediments by implementing different formulations for erosion or deposition or both and concentration-dependent settling velocities. A depth-dependence of the erodibility and critical erosion rate, which is an important characteristic of cohesive beds, is as yet rarely fully implemented. In addition, most area models still do not fully consider important cohesive processes such as turbulence-induced flocculation and break up. ECOMSED is the exception since it does relate the settling velocity to both the suspended concentration and the water column shear rate.

5.2. Empiricism

[59] A very important characteristic of the present state-of-the-art in sediment transport modeling is its high degree of empiricism. This is common for subgrid-scale processes and arises in coastal area models from turbulence, near-bed hydrodynamics, and sediment transport. All three are complex problems in coastal environments for which there are no analytical solutions and to which direct numerical solutions are still prohibitively expensive. This results in the need for parameterizations and simplifications, which unfortunately only offer a partial description of the physics and exhibit a limited range of applicability in real world scenarios. Turbulence closures in coastal area models usually employ some Reynolds-averaged Navier-Stokes model, which inherently involves some degree of empiricism. This is further com-

pounded by the near-bed sediment transport models (e.g., bed load transport equations) as well as expressions representing the interactions between sediment and turbulence (e.g., size and settling velocity of flocs of cohesive sediments).

[60] A direct consequence of the implementation of empirical formulas and/or of following simple physical assumptions concerns the range of applicability of the models. Most formulations are still unable to fully describe natural conditions. They also often need to be calibrated by experimental means, which always involve some degree of specificity with respect to the underlying conditions. For example, *Davies et al.* [2002] highlight the need for knowledge of on-site conditions in order to obtain reasonable predictions. Addressing this problem is far from being cheap and simple as it would require extensive model-data comparisons and theoretical work to reduce the degree of empiricism.

[61] Another issue at stake here is the mismatch between model outputs, such as three-dimensional sediment concentration and two-dimensional bed evolution, and the experimental data available. Experimental techniques used in coastal oceans only give a partial description of the fully three-dimensional problem. Techniques commonly used range from point measurements obtained through acoustic Doppler velocimeter to vertical profiles at a specific location with instruments such as acoustic backscatter systems for sediment concentration profiles and acoustic Doppler current profilers and coherent Doppler velocity profilers for current and velocity profiles. Spatial variations in the horizontal plane can be obtained for surface currents from HF radar measurements, and two-dimensional bathymetric changes in shallow water can be inferred from a depth inversion technique on X-band radar data [*Bell et al.*, 2006]. However, experimental data do not in general include both vertical structures and horizontal variations, and model-data comparisons necessary for three-dimensional sediment transport hindcasting remain difficult.

[62] This in turn emphasizes the need for better process-based modeling to reduce present uncertainties. While recent advances in experimental techniques provide better descriptions of the small-scale processes [e.g., *Davies and Thorne*, 2008], a mismatch between quantities measured and quantities requiring modeling at the larger scale often remains. We believe this gap between process experiments and coastal area modeling highlights the need for small-scale process modeling validated using measurements to represent the appropriate physical processes.

5.3. Turbulence Modeling

[63] Sediment transport is commonly split between suspended load and bed load. The first is commonly considered to be the part of the total load for which the dominant suspension mechanism results from the agitation of turbulence. Bed load, as mentioned in section 3.2, is due to interparticle interactions in a thin near-bed region and is commonly taken to be determined almost exclusively by the bed shear stress. The influence of turbulence closure schemes on suspended sediment transport is straightforward and has been observed by *Warner et al.* [2005], where different turbulence closures lead to significantly different suspended sediment concentration profiles. However, the effect of turbulence closures on sediment transport is really twofold as the bed shear stress is not independent of the closure used, as implied by near-bed turbulence intensities depending on the closure [e.g., *Warner et al.*, 2005].

[64] So far, coastal ocean models have used RANS turbulence models, which usually provide some description of the velocity-velocity and velocity-scalar covariances by introducing the eddy viscosity and scalar diffusivities. The eddy viscosity ν_t and diffusivities K_t are in turn calculated from a velocity scale $k^{1/2}$, where k is the turbulent kinetic energy, and a length scale l:

$$\nu_t = c_\mu k^{1/2} l \quad \text{and} \quad K_t = c'_\mu k^{1/2} l \tag{14}$$

where the quantities c_μ and c'_μ are typically referred to as the stability functions. Turbulence models in coastal area models can obtain the velocity scale and the length scale (1) both from algebraic relations, (2) from a transport equation for the energy (square of the velocity) and an algebraic relation for the length scale [e.g., *Souza et al.*, 2007], or (3) from two transport equations such as in the level 2.5 model of *Mellor and Yamada* [1982], the k-ε model [*Rodi*, 1987], or the k-ω model [*Wilcox*, 1993; *Umlauf et al.*, 2003], where ε is the turbulence dissipation rate and ω is the turbulence frequency. The stability functions can also be specified (1) as constants, (2) as empirical algebraic functions, or (3) from simplified forms of Reynolds stress models [e.g., *Canuto et al.*, 2001]. Even though all these models involve some empiricism, they can usually be applied to a wide range of turbulent flow, and their accuracy has been studied and compared in several studies [e.g., *Umlauf and Burchard*, 2003; *Warner et al.*, 2005; *Holt and Umlauf*, 2008]. The main drawback lies in the loss of information resulting from the averaging and is thus inherent to the RANS approach.

[65] In contrast, both direct numerical simulation (DNS) and large-eddy simulation (LES) solve equations for time-dependent variables for one realization of the turbulent flow. DNS consists of solving the equations of motion and resolving all scales with appropriate initial and boundary conditions. When applied, DNS provides an unmatched level of description and accuracy and is valuable in procuring information on turbulence that is impossible to obtain experimentally. However, the computational cost of DNS increases rapidly with the Reynolds number [*Pope*, 2000] making geophysical applications prohibitively expensive. Almost all this cost is due to resolving the dissipation range [*Pope*, 2000], and LES aims to avoid such expensive calculations while maintaining a high level of description. In LES, the dynamics of the larger-scale, three-dimensional unsteady turbulent motions are thus explicitly computed, whereas the small-scale effects are modeled. Compared with RANS models, LES closures will more accurately describe problems where large-scale unsteadiness is significant but are also significantly more expensive. Figure 9 presents the comparison between LES and RANS approaches for the
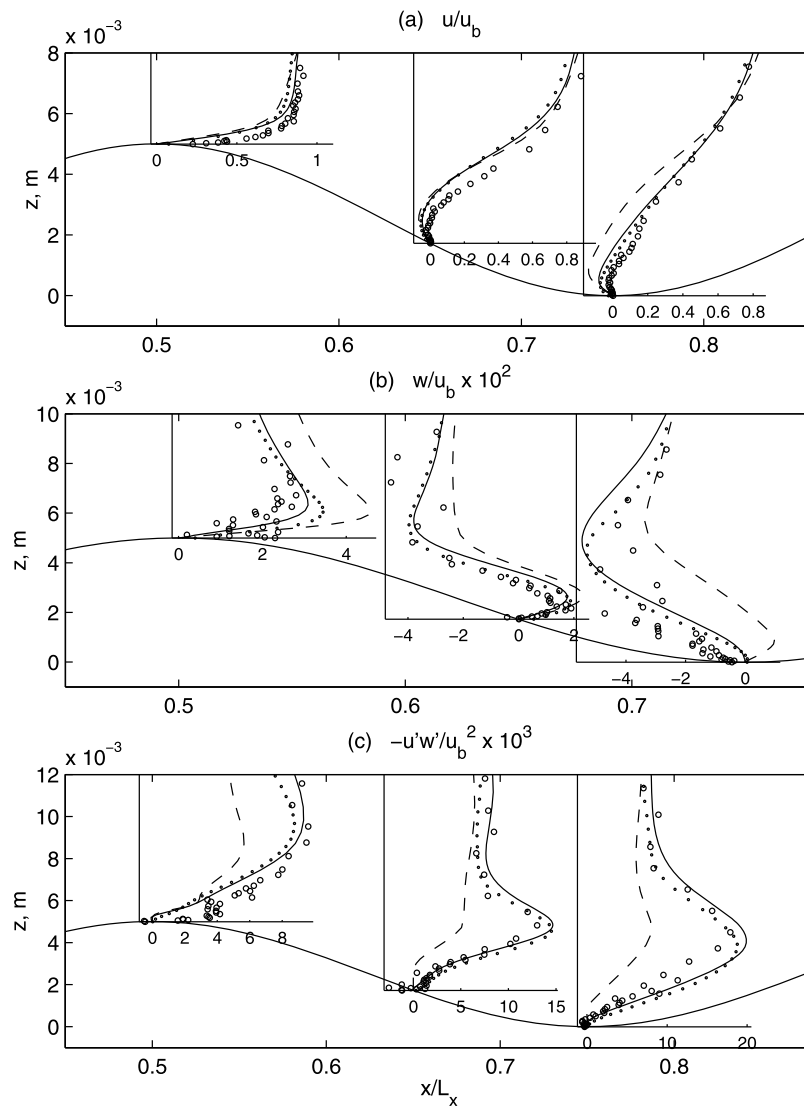
Figure 9. Comparison of turbulent flow over a ripple between experimental data (large circles), DNS data (small circles), LES (solid line), and RANS (dashed line) at three locations along the ripple: (a) mean streamwise velocity, (b) mean vertical velocity, and (c) Reynolds stress [after *Chang and Scotti*, 2004].

turbulent flow over a ripple. For wall-bounded flows, near-wall resolution still remains unfeasible because of the computational cost incurred. Instead, near-wall modeling is employed for which the near-wall energy containing scale is not resolved. The effects of the unresolved motions are then usually modeled through the use of boundary conditions similar to those used in RANS models [*Pope*, 2000].

5.4. Model Uncertainty

[66] It is particularly important at this point to realize that even the most advanced model to date can only predict sediment transport within a factor of two at best and that higher uncertainties are not uncommon. These are due in part to the strong amplification of any small errors in the hydrodynamics, which is easily explained by the power dependence of the sediment transport rates on the flow velocities (power three for the bed load transport rate and a power higher than three for the suspended load). A number

of other factors contribute to the overall uncertainty. Most importantly, no model currently combines the most advanced methods for all numerical and physical aspects (e.g., Tables 2 and 3). Many processes are insufficiently represented by empirical expressions or neglected altogether. We already mentioned that biological effects on sediment transport are missing in the sediment transport models reviewed. Another consistent simplification is the representation of the continuous sediment size distribution by, at best, a series of discrete values. Present sediment transport and morphological models also rely on the specification of physical parameters which themselves exhibit large variability and uncertainty. For example, m in equation (8) can vary by up to one order of magnitude (Table 1), E_0 can vary by several orders of magnitude, and the critical stress by one order of magnitude [*Winterwerp and van Kesteren*, 2004]. Sensitivity analyses show the dramatic effect that this variability has on the model's predictions [e.g., *Amoudry and Souza*, 2011].

[67] It is, however, an oversimplification to consider that the uncertainty is solely due to modeling issues. Model predictions need hindcasting and require numerous detailed inputs, which are often site specific. These requirements depend inherently on high-quality and extensive experimental data, which are still seldom available. In particular, large-scale bathymetries are typically the composite of several surveys conducted at sometimes significant time intervals. Bed composition data usually consist of a collection of point measurements which may not be sufficient in a highly variable environment. Both therefore present a significant challenge for obtaining an accurate initial bed condition (bathymetry and composition) on which predictions naturally depend. Overall, the uncertainty in numerical results can be significant and has many sources. It is inherently case and site specific, and we would therefore recommend that modeling studies include a sensitivity analysis and assessment of their particular uncertainty.

6. FUTURE PERSPECTIVES

[68] Even though the level of description and the accuracy of sediment transport models have greatly improved over the last few decades, some important issues remain for the aim of better regional sediment predictions. For example, several problems such as biological effects on sediment dynamics, the impact of mixed beds, and even several cohesive sediment physical processes (e.g., flocculation) are still largely ignored at the regional scale. Many other issues are lacking in terms of accuracy and/or range of applicability. Parameterizations of erosion rates for both cohesive and noncohesive sediments are insufficient both in terms of level of description of the physical processes and in terms of validation. Bed load transport rate expressions are fairly speculative for noncoarse (diameter less than around 200–300 μm) sediments. The description of wave-current interactions is incomplete, especially in terms of the range of applicability necessary to represent realistic field conditions. Ripple and roughness predictors, which are crucial for the feedback between sediment dynamics and hydrodynamics, lack appropriate physical descriptions, range of applicability, and validation. All these issues combine to limit the present predictive ability of regional models.

[69] Sediment transport presents a particular dichotomy between large-scale governing equations based on simple and well-understood principles (conservation of mass) and small-scale processes that are neither simple nor well understood. Representing these small-scale processes is the real challenge and accounts for the bulk of the effort already made and still to be made. This enterprise requires both experimental work and small-scale models focused on specific physical processes. Poor near-bed and small-scale parameterizations are commonly blamed for the performance of coastal regional models because of the large variability resulting from the different modeling approaches [e.g., *Grasmeijer et al.*, 2005; *Walstra et al.*, 2005]. It should thus come as no surprise that further process studies, both experimental and numerical, will be pivotal to improving our

predictive abilities. In particular, parameterizations of the turbulence sediment interaction (e.g., sediment diffusivity) and near-bed processes such as erosion flux and bed shear stress fail to represent the complexity of all the processes involved. Bed load modeling, in spite of an apparent consensus, still presents large uncertainties and can fail profoundly to reproduce field observations [*Kleinhans and Grasmeijer*, 2006]. Issues also arise from the quantities typically parameterized in coastal regional models being difficult to measure directly and accurately (e.g., erosion and roughness). This results in a gap between measurement outputs and regional coastal parameterizations which may be overcome via use of recent advanced small-scale process models. For example, recent sheet flow models have provided new means to estimate the bed load transport rate [e.g., *Malarkey et al.*, 2003; *Amoudry and Liu*, 2010] and the erosion rate [e.g., *Amoudry and Liu*, 2010].

[70] Another rather general shortcoming of morphological and regional coastal sediment transport models concerns the treatment of cohesive sediments. Processes such as flocculation and consolidation are rarely incorporated in regional models, and empirical formulas not always supported by sound explanations of the physical processes involved are still commonly used. Historically, the investigations that led to the various conceptual and mathematical representations used have been carried out for noncohesive and cohesive sediments separately. Some recent studies have since shown that some of the sediment dynamics' characteristics can change dramatically when cohesive and noncohesive sediments are mixed. For example, *Mitchener and Torfs* [1996] found that the erosion was dramatically changed when mud is added to sand. Such issues arising from mixed sediments (all of cohesive-cohesive, cohesive-noncohesive, and noncohesive-noncohesive mixtures) are currently only partially understood and not included in regional models. Implementing such cohesive and mixed sediment processes thus represents an important challenge for modelers aiming to predict sediment dynamics in coastal and estuarine environments.

[71] Finally, even though biological and sediment transport models have each been coupled to coastal ocean modeling systems, biological effects on sediment transport are still generally not included in deterministic coastal area sediment transport models. This presents a significant shortcoming for predictions as biological effects have been shown to modify some sediment processes and near-bed hydrodynamics. For example, the bottom boundary layer may be significantly impacted by the presence of living organisms via the introduction of a nonnegligible biogenic roughness [e.g., *Wheatcroft*, 1994]. Sediment bed erosion can also exhibit important variability due to biological controls [e.g., *Defew et al.*, 2002; *Stevens et al.*, 2007]. Biology may affect sediment erosion via stabilizing or destabilizing processes. Microphytobenthos can increase the erosion threshold [e.g., *Lelieveld et al.*, 2003] via production of extracellular polymeric substances, while macrofaunal species can increase sediment erodibility via bioturbation [e.g., *Widdows et al.*, 2009]. Near-bed hydrodynamic and sediment erosion are

not the only processes impacted, and organic matter and living microorganisms are also an important control on flocculation processes [*Maggi*, 2009].

[73] The Editor on this paper was Eelco Rohling. He thanks reviewer Carl Amos and two other anonymous reviewers.

REFERENCES

Ahilan, R. V., and J. F. A. Sleath (1987), Sediment transport in oscillatory flow over flat bed, *J. Hydraul. Eng.*, *113*(3), 308–322.

Amoudry, L. O., and P. L.-F. Liu (2009), Two-dimensional, two-phase granular sediment transport model with applications to scouring downstream of an apron, *Coastal Eng.*, *56*, 693–702, doi:10.1016/j.coastaleng.2009.01.006.

Amoudry, L. O., and P. L.-F. Liu (2010), Parameterization of near-bed processes under collinear wave and current flows from a two-phase sheet flow model, *Cont. Shelf Res.*, *30*, 1403–1416.

Amoudry, L. O., and A. J. Souza (2011), Impact of sediment-induced stratification and turbulence closures on sediment transport and morphological modelling, *Cont. Shelf Res.*, *31*, 912–928.

Amoudry, L., T.-J. Hsu, and P. L.-F. Liu (2005), Schmidt number and near-bed boundary condition effects on a two-phase dilute sediment transport model, *J. Geophys. Res.*, *110*, C09003, doi:10.1029/2004JC002798.

Ariathurai, R., and R. B. Krone (1976), Finite element model for cohesive sediment transport, *J. Hydraul. Div. Am. Soc. Civ. Eng.*, *102*(3), 323–338.

Bagnold, R. A. (1954), Experiments on a gravity-free dispersion of large solid spheres in a newtonian fluid under shear, *Philos. Trans. R. Soc. London A*, *225*, 49–63.

Bagnold, R. A. (1966), An approach to the sediment transport problem from general physics, *U.S. Geol. Surv. Prof. Pap.*, *422-I*, 44 pp.

Bailard, J. A. (1981), An energetics total load sediment transport model for a plane sloping beach, *J. Geophys. Res.*, *86*(C11), 10,938–10,954.

Bell, P. S., J. J. Williams, S. Clark, B. D. Morris, and A. Vila-Concejo (2006), Nested radar systems for remote coastal observations, *J. Coastal Res. Spec. Issue*, *39*, 483–487.

Bijker, E. W. (1969), Littoral drift as function of waves and current, in *Proceedings of 11th Conference on Coastal Engineering*, pp. 415–435, Am. Soc. of Civ. Eng., Reston, Va.

Blaas, M., C. Dong, P. Marchesiello, J. C. McWilliams, and K. D. Stolzenbach (2007), Sediment-transport modeling on Southern Californian shelves: A ROMS case study, *Cont. Shelf Res.*, *27*, 832–853.

Blumberg, A. F. (2002), *A Primer for ECOMSED, Version 1.3*, users manual, HydroQual, Inc., Mahwah, N. J.

Blumberg, A. F., and G. L. Mellor (1987), A description of a three-dimensional coastal ocean circulation model, in *Three-Dimensional Coastal Ocean Models*, *Coastal Estuarine Sci.*, vol. 4, edited by N. S. Heaps, pp. 1–16, AGU, Washington, D. C.

Booij, N., R. C. Ris, and L. H. Holthuijsen (1999), A third-generation wave model for coastal regions: 1. Model description and validation, *J. Geophys. Res.*, *104*(C4), 7649–7666.

Briand, M.-H. G., and J. W. Kamphuis (1993), Sediment transport in the surf zone: A quasi 3-D numerical model, *Coastal Eng.*, *20*, 135–156.

Brocchini, M., and T. Baldock (2008), Recent advances in modeling swash zone dynamics: Influence of surf-swash interaction on nearshore hydrodynamics and morphodynamics, *Rev. Geophys.*, *46*, RG3003, doi:10.1029/2006RG000215.

Brown, J. M., and A. G. Davies (2009), Methods for medium-term prediction of the net sediment transport by waves and currents in complex coastal regions, *Cont. Shelf Res.*, *29*, 1502–1514.

Burban, P.-Y., Y.-J. Xu, J. McNeil, and W. Lick (1990), Settling speeds of flocs in fresh water and seawater, *J. Geophys. Res.*, *95*(C10), 18,213–18,220.

Burchard, H., K. Bolding, and M. R. Villarreal (2004), Three-dimensional modelling of estuarine turbidity maxima in a tidal estuary, *Ocean Dyn.*, *54*(2), 250–265.

Burchard, H., G. Flöser, J. V. Staneva, T. H. Badewien, and R. Riethüller (2008), Impact of density gradients on net sediment transport into the Wadden Sea, *J. Phys. Oceanogr.*, *38*, 566–587.

Byun, D.-S., and X. H. Wang (2005), The effect of sediment stratification on tidal dynamics and sediment transport patterns, *J. Geophys. Res.*, *110*, C03011, doi:10.1029/2004JC002459.

Canuto, V. M., A. Howard, Y. Cheng, and M. S. Dubovikov (2001), Ocean turbulence. Part I: One-point closure model—Momentum and heat vertical diffusivities, *J. Phys. Oceanogr.*, *31*, 1413–1426.

Celik, I., and W. Rodi (1988), Modelling suspended sediment transport in non-equilibrium situations, *J. Hydraul. Eng.*, *114*(10), 1157–1191.

Chang, Y. S., and A. Scotti (2004), Modeling unsteady turbulent flows over ripples: Reynolds-averaged Navier-Stokes equations (RANS) versus large-eddy simulation (LES), *J. Geophys. Res.*, *109*, C09012, doi:10.1029/2003JC002208.

Chen, C., H. Liu, and R. C. Beardsley (2003), An unstructured grid, finite-volume, three-dimensional, primitive equations ocean model: Application to coastal ocean and estuaries, *J. Atmos. Oceannic Technol.*, *20*, 159–186.

Chen, C., H. Huang, R. C. Beardsley, H. Liu, Q. Xu, and G. Cowles (2007), A finite volume numerical approach for coastal ocean circulation studies: Comparisons with finite difference models, *J. Geophys. Res.*, *112*, C03018, doi:10.1029/2006JC003485.

Cookman, J. L., and P. B. Flemings (2001), STORMSED 1.0: Hydrodynamics and sediment transport in a 2-D, steady-state, wind-and wave-driven coastal circulation model, *Comput. Geosci.*, *27*(6), 647–674.

Damgaard, J., R. J. S. Whitehouse, and R. L. Soulsbby (1997), Bed-load sediment transport on steep longitudinal slopes, *J. Hydraul. Eng.*, *123*(12), 1130–1138.

Damgaard, J., N. Dodd, L. Hall, and T. Chesher (2002), Morphodynamic modelling of rip channel growth, *Coastal Eng.*, *45*, 199–221.

Davies, A. G., and P. D. Thorne (2008), Advances in the study of moving sediments and evolving seabeds, *Surv. Geophys.*, *29*, 1–36.

Davies, A. G., and C. Villaret (2000), Sand transport by waves and currents: predictions of research and engineering methods, in *Proceedings of the 27th Conference on Coastal Engineering, Sydney, Australia, 2000*, edited by B. L. Edge, pp. 2481–2494, Am. Soc. of Civ. Eng., Reston, Va.

Davies, A. G., L. C. van Rijn, J. S. Damgaard, J. van der Graaff, and J. S. Ribberink (2002), Intercomparison of research and practical sand transport models, *Coastal Eng.*, *46*, 1–23.

de Vriend, H. J. (1987), 2DH mathematical modelling of morphological evolutions in shallow water, *Coastal Eng.*, *11*, 1–27.

de Vriend, H. J., and J. S. Ribberink (1988), A quasi-3D mathematical model of coastal morphology, in *Procedings of the 21st International Conference on Coastal Engineering*, edited by B. L. Edge, pp. 1689–1703, Am. Soc. of Civ. Eng., Reston, Va.

de Vriend, H. J., J. Zyserman, J. Nicholson, J. A. Roelvink, P. Pechon, and H. N. Southgate (1993), Medium term 2DH coastal modelling, *Coastal Eng.*, *21*, 193–224.

Defew, E. C., T. J. Tolhurst, and D. M. Paterson (2002), Site-specific features influence sediment stability of intertidal flats, *Hydrol. Earth Syst. Sci.*, *6*(6), 971–982.

Deigaard, R., J. Fredsøe, and I. B. Hedegaard (1986), Suspended sediment in the surf zone, *J. Waterw. Port Coastal Ocean Eng.*, *112*(1), 115–128.

Delft Hydraulics (2007), *Delft3D-FLOW: Simulation of multi-dimensional hydrodynamic flows and transport phenomema, including sediments*, user manual, Deltares, Delft, Netherlands.

Delo, E. A. (1988), Estuarine muds manual, *Rep. SR 164*, Hydraul. Res., Ltd., Wallingford, U. K.

DHI (2004), MIKE 21 wave modelling: MIKE 21 SW - Spectral waves FM. Short description, report, Hørsholm, Denmark.

DHI (2006), MIKE 21 and MIKE 3 Flow Model FM: Hydrodynamic module. Short description, report, Hørsholm, Denmark.

DHI (2007a), MIKE 21 and MIKE 3 Flow Model FM: Sand transport module. Short description, report, Hørsholm, Denmark.

DHI (2007b), MIKE 21 and MIKE 3 Flow Model FM: Mud transport module. Short description, report, Hørsholm, Denmark.

Dibajnia, M., and A. Wanatabe (1992), Sheet flow under nonlinear waves and currents, in *Proceedings of the 23rd International Conference on Coastal Engineering*, edited by B. L. Edge, pp. 2015–2028, Am. Soc. of Civ. Eng., Reston, Va.

Dyer, K. R., and A. J. Manning (1999), Observation of the size, settling velocity and effective density of flocs and their fractal dimensions, *J. Sea Res.*, *41*, 87–95.

Einstein, H. A. (1950), The bed-load function for sediment transportation in open channel flows, *Tech. Bull. 1026*, Soil Conserv. Serv., U.S. Dept. of Agric., Washington, D. C.

Elfrink, B., I. Broker, R. Deigaard, E. A. Hansen, and P. Justesen (1996), Modelling of 3D sediment transport in the surf zone, in *Proceedings of the 25th International Conference on Coastal Engineering*, edited by B. L. Edge, pp. 3805–3817, Am. Soc. of Civ. Eng., Reston, Va.

Elias, E., and G. Gelfenbaum (2009), Modeling processes controlling sediment transport at the mouth of the Columbia River, in *Proceedings of Coastal Dynamics 2009: Impacts of Human Activities on Dynamic Coastal Processes*, edited by M. Mizuguchi and S. Sato, pp. 1–14, World Sci., Hackensack, N. J.

Engelund, F., and J. Fredsøe (1976), A sediment transport model for straight alluvial channels, *Nord. Hydrol.*, *7*, 293–306.

Engelund, F., and E. Hansen (1967), A monograph on sediment transport in alluvial streams, technical report, Hydraul. Lab., Denmark Tech. Univ., Copenhagen.

Fang, H. W., and W. Rodi (2003), Three-dimensional calculations of flow and suspended sediment transport in the neighborhood of the dam for the Three Gorges Project (TGP) reservoir in the Yangtze River., *J. Hydraul. Res.*, *41*(4), 379–394.

Fernandez Luque, R., and R. van Beek (1976), Erosion and transport of bed-load sediment, *J. Hydraul. Res.*, *14*(2), 127–144.

Fredsøe, J. (1984), Turbulent boundary layer in wave-current motion, *J. Hydraul. Eng.*, *110*(8), 1103–1120.

Fredsøe, J., and R. Deigaard (1992), *Mechanics of Coastal Sediment Transport*, World Sci., Singapore.

Fredsøe, J., O. H. Andersen, and S. Silberg (1985), Distribution of suspended sediment in large waves, *J. Waterw. Port Coastal Ocean Eng.*, *111*(6), 1041–1059.

Garcia, M., and G. Parker (1991), Entrainment of bed sediment into suspension, *J. Hydraul. Eng.*, *117*(4), 414–435.

Gessler, D., B. Hall, M. Spasojevic, F. Holly, H. Pourtaheri, and N. Raphelt (1999), Application of 3D Mobile Bed, Hydrodynamic Model, *Coastal Eng.*, *125*, 737–749.

Gibson, R. E., G. L. England, and M. J. L. Hussey (1967), The theory of one-dimensional consolidation of saturated clays, *Geotechnique*, *17*, 261–273.

Graf, W. H., and M. Cellino (2002), Suspension flows in open channels; experimental study, *J. Hydraul. Res.*, *40*(4), 435–447.

Grant, W. D., and O. S. Madsen (1979), Combined wave and current interaction with a rough bottom, *J. Geophys. Res.*, *84*(C4), 1797–1808.

Grant, W. D., and O. S. Madsen (1982), Movable bed roughness in unsteady oscillatory flow, *J. Geophys. Res.*, *87*(C1), 469–481.

Grant, W. D., and O. S. Madsen (1986), The continental-shelf bottom boundary layer, *Annu. Rev. Fluid Mech.*, *18*(1), 265–305.

Grasmeijer, B. T., A. G. Davies, K. Guizien, J. J. van der Werf, L. C. van Rijn, R. Walther, J. Sutherland, and J. Biegowski (2005), Intercomparison results of sand transport models based on blind benchmarking test cases, in *SANDPIT: Sand Transport and Morphology of Offshore Sand Mining Pits*, edited by L. C. van Rijn et al., pp. AM1–AM10, Aqua Publ., Blokzijl, Netherlands.

Haidvogel, D. B., et al. (2008), Ocean forecasting in terrain-following coordinates: Formulation and skill assessment of the regional ocean modeling system, *J. Comput. Phys.*, *227*, 3595–3624.

Harris, C. K., and P. L. Wiberg (2001), A two-dimensional, time-dependent model of suspended sediment transport and bed reworking for continental shelves, *Comput. Geosci.*, *27*(6), 675–690.

Harris, C. K., C. R. Sherwood, R. P. Signell, A. J. Bever, and J. C. Warner (2008), Sediment dispersal in the northwestern Adriatic Sea, *J. Geophys. Res.*, *113*, C11S03, doi:10.1029/2006JC003868.

Hill, P. S., A. R. M. Nowell, and P. A. Jumars (1988), Flume evaluation of the relationship between suspended sediment concentration and excess boundary shear stress, *J. Geophys. Res.*, *93*(C10), 12,499–12,509.

Holt, J., and L. Umlauf (2008), Modelling the tidal mixing fronts and seasonal stratification of the northwest European continental shelf, *Cont. Shelf Res.*, *28*, 887–903.

Hsu, T.-J., J. T. Jenkins, and P. L.-F. Liu (2004), On two-phase sediment transport: sheet flow of massive particles, *Philos. Trans. R. Soc. London A*, *460*, 2223–2250, doi:10.1098/rspa.2003.1273.

Hsu, T.-J., S. Elgar, and R. T. Guza (2006), Wave-induced sediment transport and onshore sandbar migration, *Coastal Eng.*, *53*, 817–824.

Hu, K., P. Ding, Z. Wang, and S. Yang (2009), A 2D/3D hydrodynamic and sediment transport model for the Yangtze Estuary, China, *J. Mar. Syst.*, *77*, 114–136.

Ikeda, S. (1982), Lateral bed load transport on side slopes, *J. Hydraul. Div. Am. Soc. Civ. Eng.*, *108*(11), 1369–1373.

Jones, O. P., O. S. Petersen, and H. Kofoed-Hansen (2007), Modeling of complex coastal environments: Some considerations for best practice, *Coastal Eng.*, *54*, 717–733.

Jonsson, I. G. (1966), Wave boundary layers and friction factors, in *Proceedings of 10th International Conference on Coastal Engineering*, pp. 127–148, Am. Soc. of Civ. Eng., Reston, Va.

Kamphuis, J. W. (1975), Friction factor under oscillatory waves, *J. Waterw. Port Coastal Ocean Eng.*, *101*(2), 135–144.

Kleinhans, M. G., and B. T. Grasmeijer (2006), Bed load transport on the shoreface by currents and waves, *Coastal Eng.*, *53*, 983–996.

Komen, G. J., L. Cavaleri, M. Donelan, K. Hasselmann, S. Hasselmann, and P. A. E. M. Janssen (1994), *Dynamics and Modelling of Ocean Waves*, Cambridge Univ. Press, New York.

Kranenburg, C. (1994), The fractal structure of cohesive sediment aggregates, *Estuarine Coastal Shelf Sci.*, *39*, 451–460.

Krone, R. B. (1962), Flume studies of the transport of sediment in estuarial shoaling processes, final report, Hydraul. Eng. and Salinity Eng. Res. Lab., Univ. of Calif., Berkeley.

Lane, A. (2005), Development of a Lagrangian sediment model to reproduce the bathymetric evolution of the Mersey Estuary, *Ocean Dyn.*, *55*(5–6), 541–548.

Lelieveld, S. D., C. A. Pilditch, and M. O. Green (2003), Variation in sediment stability and relation to indicators of microbial abundance in the Okura Estuary, New Zealand, *Estuarine Coastal Shelf Sci.*, *57*, 123–136.

Lesser, G., J. van Kester, and J. A. Roelvink (2000), On-line sediment transport within Delft3D-FLOW, Rep. Z2396, WL Delft Hydraul., Delft, Netherlands.

Lesser, G. R., J. A. Roelvink, J. van Kester, and G. S. Stelling (2004), Development and validation of a three-dimensional morphological model, *Coastal Eng.*, *51*, 883–915.

Li, M. Z., and C. L. Amos (1998), Predicting ripple geometry and bed roughness under combined waves and currents in a continental shelf environment, *Cont. Shelf Res.*, *18*, 941–970.

Li, M. Z., and C. L. Amos (2001), SEDTRANS96: the upgraded and better calibrated sediment-transport model for continental shelves, *Comput. Geosci.*, *27*(6), 619–645.

Lick, W., H. Huang, and R. Jepsen (1993), Flocculation of fine grained sediments due to differential settling, *J. Geophys. Res.*, *98*(C6), 10,279–10,288.

Lumborg, U. (2005), Modelling the deposition, erosion, and flux of cohesive sediment through Øresund, *J. Mar. Syst.*, *56*, 179–193.

Lumborg, U., and A. Windelin (2003), Hydrography and cohesive sediment modelling: application to the Rømø Dyb tidal area, *J. Mar. Syst.*, *38*, 287–303.

Madsen, O. S. (1994), Spectral wave-current bottom boundary layer flows, in *Proceedings of the 24th International Conference on Coastal Engineering*, edited by B. L. Edge, pp. 384–398, Am. Soc. of Civ. Eng., Reston, Va.

Maggi, F. (2009), Biological flocculation of suspended particles in nutrient-rich aqueous ecosystems, *J. Hydrol.*, *376*, 116–125.

Malarkey, J., and A. G. Davies (2003), A non-iterative procedure for the Wiberg and Harris (1994) oscillatory sand ripple predictor, *J. Coastal Res.*, *19*, 738–739.

Malarkey, J., A. G. Davies, and Z. Li (2003), A simple model of unsteady sheet-flow sediment transport, *Coastal Eng.*, *48*, 171–188.

Manning, A. J., and K. R. Dyer (1999), A laboratory examination of floc characteristics with regard to turbulent shearing, *Mar. Geol*, *160*, 147–170.

Mehta, A. J. (1986), Characterization of cohesive sediment transport processes in estuaries, in *Estuarine Cohesive Sediment Dynamics*, edited by A. J. Mehta, pp. 290–325, Springer, Berlin.

Mehta, A. J., E. J. Hayter, W. R. Parker, R. B. Krone, and A. M. Teeter (1989), Cohesive sediment transport. I: Process description, *J. Hydraul. Eng.*, *115*(8), 1076–1093.

Mei, C. C., S. J. Fan, and K. R. Jin (1997), Resuspension and transport of fine sediments by waves, *J. Geophys. Res.*, *102*(C7), 15,807–15,821.

Mellor, G. (2002), Oscillatory bottom boundary layers, *J. Phys. Oceanogr.*, *32*, 3075–3088.

Mellor, G., and T. Yamada (1982), Development of a turbulence closure model for geophysical fluid problems, *Rev. Geophys.*, *20*(4), 851–875.

Meyer-Peter, E., and R. Müller (1948), Formulas for bed-load transport, paper presented at 2nd Meeting of International Association for Hydraulic Research, Int. Assoc. for Hydraul. Res., Stockholm.

Mitchener, H., and H. Torfs (1996), Erosion of mud/sand mixtures, *Coastal Eng.*, *29*, 1–25.

Mogridge, G. R., M. H. Davies, and D. H. Willis (1994), Geometry prediction for wave-generated bedforms, *Coastal Eng.*, *22*, 255–286.

Neumeier, U., C. Ferrarin, C. L. Amos, G. Umgiesser, and M. Z. Li (2008), Sedtrans05: An improved sediment-transport model for continental shelves and coastal waters with a new algorithm for cohesive sediments, *Comput. Geosci.*, *34*(10), 1223–1242, doi:10.1016/j.cageo.2008.02.007.

Nielsen, P. (1981), Dynamics and geometry of wave-generated ripples, *J. Geophys. Res.*, *86*(C7), 6467–6472.

Nielsen, P. (1992), *Coastal Bottom Boundary Layers and Sediment Transport*, World Sci., Singapore.

O'Donoghue, T., J. S. Doucette, J. J. van der Werf, and J. S. Ribberink (2006), The dimensions of sand ripples in full-scale oscillatory flows, *Coastal Eng.*, *53*, 997–1012.

Pandoe, W. W., and B. L. Edge (2004), Cohesive sediment transport in the 3D-hydrodynamic-baroclinic circulation model: Study case for idealized tidal inlet, *Ocean Eng.*, *31*, 2227–2252.

Paola, C., and V. R. Voller (2005), A generalized Exner equation for sediment mass balance, *J. Geophys. Res.*, *110*, F04014, doi:10.1029/2004JF000274.

Pope, S. B. (2000), *Turbulent Flows*, 1st ed., Cambridge Univ. Press, New York.

Rakha, K. A., R. Deigaard, and I. Brøker (1997), A phase-resolving cross shore sediment transport model for beach profile evolution, *Coastal Eng.*, *31*, 231–261.

Ribberink, J. S. (1998), Bed-load transport for steady flows and unsteady oscillatory flows, *Coastal Eng.*, *34*, 59–82.

Richardson, J. F., and W. N. Zaki (1954), Sedimentation and fluidization, *Trans. Inst. Chem. Eng.*, *32*, 35–53.

Rodi, W. (1987), Examples of calculation methods for flow and mixing in statified fluids, *J. Geophys. Res.*, *92*(C5), 5305–5328.

Roelvink, J. A., D. J. R. Walstra, and Z. Chen (1994), Morphological modelling of Keta Lagoon case, in *Proceedings of the 24th International Conference on Coastal Engineering*, edited by B. L. Edge, pp. 3223–3236, Am. Soc. of Civ. Eng., Reston, Va.

Rose, C. P., and P. D. Thorne (2001), Measurements of suspended sediment transport parameters in a tidal estuary, *Cont. Shelf Res.*, *21*, 1551–1575.

Safak, I., A. Sheremet, M. A. Allison, and T.-J. Hsu (2010), Bottom turbulence on the muddy Atchafalaya Shelf, Louisiana, USA, *J. Geophys. Res.*, *115*, C12019, doi:10.1029/2010JC006157.

Sanford, L. P. (2008), Modeling a dynamically varying mixed sediment bed with erosion, deposition, bioturbation, consolidation, and armoring, *Comput. Geosci.*, *34*(10), 1263–1283, doi:10.1016/j.cageo.2008.02.011.

Sanford, L. P., and J. P. Halka (1993), Assessing the paradigm of mutually exclusive erosion and deposition of mud, with examples from upper Chesapeake bay, *Mar. Geol.*, *114*, 37–57.

Sanford, L. P., and J. P.-Y. Maa (2001), A unified erosion formulation for fine sediments, *Mar. Geol.*, *179*, 9–23.

Sekine, M., and G. Parker (1992), Bed-load transport on transverse slope, *J. Hydraul. Eng.*, *118*(4), 513–535.

Shields, I. A. (1936), Anwendung der Aehnlichkeitsmechanik und der Turbulenzforschung auf die Geschiebebewegung, *Mitt. Preuss. Versuchsanst. Wasserbau Schiffbau 26*, Tech. Univ. Berlin, Berlin.

Smagorinsky, J., S. Manabe, and J. L. Holloway (1965), Numerical results from and nine-level general circulation model of the atmosphere, *Mon. Weather Rev.*, *93*(12), 727–768.

Smith, J. D., and S. R. McLean (1977), Spatially averaged flow over a wavy surface, *J. Geophys. Res.*, *82*(12), 1735–1746.

Soulsby, R. L. (1987), Calculating bottom orbital velocity beneath waves, *Coastal Eng.*, *11*, 371–380.

Soulsby, R. L. (1995), Bed shear-stresses due to combined waves and currents, in *Advances in Coastal Morphodynamics: An Overview of the G8-Coastal Morphodynamics Project*, edited by M. J. F. Stive et al., pp. 4.20–4.23, Delft Hydraul., Delft, Netherlands.

Soulsby, R. L. (1997), *Dynamics of Marine Sands: A Manual for Practical Applications*, Thomas Telford, London.

Soulsby, R. L., and S. Clarke (2005), Bed shear-stresses under combined waves and currents on smooth and rough beds, *Rep. TR 137*, Hydraul. Res., Ltd., Wallingford, U. K.

Soulsby, R. L., and J. S. Damgaard (2005), Bedload sediment transport in coastal waters, *Coastal Eng.*, *52*, 673–689.

Soulsby, R. L., and R. J. S. Whitehouse (2005), Prediction of ripple properties in shelf seas, *Rep. TR 154*, Hydraul. Res., Ltd., Wallingford, U. K.

Soulsby, R. L., L. Hamm, G. Klopman, D. Myrhaug, R. R. Simons, and G. P. Thomas (1993), Wave-current interaction within and outside the bottom boundary layer, *Coastal Eng.*, *21*, 41–69.

Souza, A. J., J. T. Holt, and R. Proctor (2007), Modelling SPM on the NW European shelf seas, in *Coastal and Shelf Sediment Transport*, edited by P. S. Balson and M. B. Collins, *Geol. Soc. Spec. Publ.*, *274*, 147–158.

Stevens, A. W., R. A. Wheatcroft, and P. L. Wiberg (2007), Seabed properties and sediment erodibility along the western Adriatic margin, Italy, *Cont. Shelf Res.*, *27*, 400–416.

Struiksma, N., K. W. Olesen, C. Flokstra, and H. J. de Vriend (1985), Bed deformation in curved alluvial channels, *J. Hydraul. Res.*, *23*(1), 57–79.

Styles, R., and S. M. Glenn (2000), Modeling stratified wave and current bottom boundary layers on the continental shelf, *J. Geophys. Res.*, *105*(C10), 24,119–24,139.

Styles, R., and S. M. Glenn (2002), Modeling bottom roughness in the presence of wave-generated ripples, *J. Geophys. Res.*, *107*(C8), 3110, doi:10.1029/2001JC000864.

Swart, D. H. (1974), Offshore sediment transport and equilibrium beach profile, *Delft Hydraul. Lab. Publ. 131*, Delft Univ. of Technol., Delft, Netherlands.

Thompson, C. E. L., C. L. Amos, M. Angelaki, T. E. R. Jones, and C. E. Binks (2006), An evaluation of bed shear stress under turbid flows, *J. Geophys. Res.*, *111*, C04008, doi:10.1029/2005JC003287.

Thorne, P. D., A. G. Davies, and P. S. Bell (2009), Observations and analysis of sediment diffusivity profiles over sandy rippled beds under waves, *J. Geophys. Res.*, *114*, C02023, doi:10.1029/2008JC004944.

Traykovski, P. (2007), Observations of wave orbital scale ripples and a nonequilibrium time-dependent model, *J. Geophys. Res.*, *112*, C06026, doi:10.1029/2006JC003811.

Umlauf, L., and H. Burchard (2003), A generic length-scale equation for geophysical turbulence models, *J. Mar. Res.*, *61*(2), 235–265.

Umlauf, L., H. Burchard, and K. Hutter (2003), Extending the k-ω turbulence model towards oceanic applications, *Ocean Modell.*, *5*, 195–218.

Unesco (1981), Tenth report of the joint panel on oceanographic tables and standards, *Unesco Tech. Pap. Mar. Sci. 36*, U. N. Educ. Sci. and Cult. Org., Paris.

van Rijn, L. C. (1984a), Sediment transport, part II: Suspended load transport, *J. Hydraul. Eng.*, *110*(11), 1613–1641.

van Rijn, L. C. (1984b), Sediment transport, part I: Bed load transport, *J. Hydraul. Eng.*, *110*(10), 1431–1456.

van Rijn, L. C. (1993), *Principles of Sediment Transport in Rivers, Estuaries and Coastal Seas*, Aqua Publ., Blokzijl, Netherlands.

Villaret, C. (2004), SISYPHE release 5.4: User's manual, *Rep. P75G17*, Lab. Natl. Hydraul. et Environ., Electr. de Fr., Chatou, France.

Villaret, C., and J. H. Trowbridge (1991), Effects of stratification by suspended sediments on turbulent shear flows, *J. Geophys. Res.*, *96*(C6), 10,659–10,680.

Villatoro, M. M., C. L. Amos, G. Umgiesser, C. Ferrarin, L. Zaggia, C. E. L. Thompson, and D. Are (2010), Sand transport measurements in Chioggia inlet, Venice lagoon: Theory versus observations, *Cont. Shelf Res.*, *30*, 1000–1018.

Wai, O. W. H., Y. Chen, and Y. S. Li (2004), A 3-D wave-current driven coastal sediment transport model, *Coastal Eng. J.*, *46*(4), 385–424.

Walstra, D. J. R., T. Chesher, A. G. Davies, J. Ribberink, P. Sergent, P. Silva, G. Vittori, R. Walther, and L. C. van Rijn (2005), Intercomparison of the state of the morphological models, in *SANDPIT: Sand Transport and Morphology of Offshore Sand Mining Pits*, edited by L. C. van Rijn et al., pp. AY1–AY23, Aqua Publ., Blokzijl, Netherlands.

Warner, J. C., C. R. Sherwood, H. G. Arango, and R. P. Signell (2005), Performance of four turbulence closure models implemented using a generic length scale method, *Ocean Modell.*, *8*, 81–113.

Warner, J. C., C. R. Sherwood, R. P. Signell, C. K. Harris, and H. G. Arango (2008), Development of a three-dimensional, regional, coupled wave, current, and sediment transport model, *Comput. Geosci.*, *34*(10), 1284–1306, doi:10.1016/j.cageo.2008.02.012.

Wheatcroft, R. A. (1994), Temporal variation in bed configuration and one-dimensional bottom roughness and the mid-shelf STRESS site, *Cont. Shelf Res.*, *14*, 1167–1190.

Whitehouse, R. (1995), Observations of the boudary layer characteristics and the suspension of sand at a tidal site, *Cont. Shelf Res.*, *15*, 1549–1567.

Whitehouse, R. J. S., R. L. Soulsby, W. Roberts, and H. J. Mitchener (2000), *Dynamics of Estuarine Muds: A Manual for Practical Applications*, Thomas Telford, London.

Wiberg, P. L., and C. K. Harris (1994), Ripple geometry in wave-dominated environments, *J. Geophys. Res.*, *99*(C1), 775–789.

Wiberg, P. L., and J. M. Nelson (1992), Unidirectional flow over asymmetric and symmetric ripples, *J. Geophys. Res.*, *97*(C8), 12,745–12,761.

Wiberg, P. L., and D. M. Rubin (1989), Bed roughness produced by saltating sediment, *J. Geophys. Res.*, *94*(C4), 5011–5016.

Wiberg, P. L., and C. R. Sherwood (2008), Calculating wave-generated bottom orbital velocities from surface-wave parameters, *Comput. Geosci.*, *34*(10), 1243–1262, doi:10.1016/j.cageo.2008.02.010.

Widdows, J., M. D. Brinsley, and N. D. Pope (2009), Effect of *Nereis diversicolor* density on the erodability of estuarine sediment, *Mar. Ecol. Prog. Ser.*, *378*, 135–143.

Wilcox, D. C. (1993), *Turbulence Modeling for CFD*, DCW Industries, La Cañada, Calif.

Wilson, K. C. (1966), Bed-load transport at high shear stress, *J. Hydraul. Div. Am. Soc. Civ. Eng.*, *92*(6), 49–59.

Winterwerp, J. C. (2001), Stratification effects by cohesive and non-cohesive sediment, *J. Geophys. Res.*, *106*(C10), 22,559–22,574.

Winterwerp, J. C. (2002), On the flocculation and settling velocity of estuarine mud, *Cont. Shelf Res.*, *22*, 1339–1360.

Winterwerp, J. C., and W. G. M. van Kesteren (2004), *Introduction to the Physics of Cohesive Sediment in the Marine Environment*, *Dev. Sedimentol.*, vol. 56, Elsevier, Amsterdam.

Winterwerp, J. C., A. J. Manning, C. Martens, T. de Mulder, and J. Vanlede (2006), A heuristic formula for turbulence-induced flocculation of cohesive sediment, *Estuarine Coastal Shelf Sci.*, *68*, 195–207.

Wu, W. (2004), Depth-averaged two-dimensional numerical modeling of unsteady flow and nonuniform sediment transport in open channels, *J. Hydraul. Eng.*, *130*(10), 1013–1024.

Wu, W., W. Rodi, and T. Wenka (2000), 3D numerical modeling of flow and sediment transport in open channels, *J. Hydraul. Eng.*, *126*(1), 4–15.

Xu, J. P., and L. D. Wright (1995), Tests of bed roughness models using field data from the Middle Atlantic Bight, *Cont. Shelf Res.*, *15*, 1409–1434.

Zanuttigh, B. (2007), Numerical modelling of the morphological response induced by low-crested structures in Lido di Dante, Italy, *Coastal Eng.*, *54*, 31–47.

Zhang, Y., D. J. P. Swift, S. Fan, A. W. Niedoroda, and C. W. Reed (1999), Two-dimensional numerical modeling of storm deposition on the northern California shelf, *Mar. Geol.*, *154*, 155–167.

Zyserman, J. A., and J. Fredsøe (1994), Data analysis of bed concentration of suspended sediment, *J. Hydraul. Eng.*, *120*(9), 1021–1042.

L. O. Amoudry and A. J. Souza, National Oceanography Centre, Joseph Proudman Bldg., 6 Brownlow St., Liverpool L3 5DA, UK. (laou@pol.ac.uk; ajso@pol.ac.uk)